

## Running head: Hemlock responses to Holocene climates

# Multivariate climate change, the climate niche, and the Holocene history of eastern hemlock (*Tsuga canadensis*)

Bryan Shuman<sup>1</sup>, W. Wyatt Oswald<sup>2</sup>, David R. Foster<sup>3</sup>

1. Department of Geology & Geophysics, University of Wyoming, Laramie WY 82071

2. Institute for Liberal Arts and Interdisciplinary Studies, Emerson College, Boston MA

3. Harvard Forest, Harvard University, Petersham MA 01366

2/12/19

Main text: 10,143 words

## Running head: Hemlock responses to Holocene climates

### 18   **Abstract** (350 words)

19   Forests in the eastern North America have changed progressively over the 11,700 years of the  
20   Holocene Epoch. To understand the dynamics involved, we focus on eastern hemlock (*Tsuga*  
21   *canadensis*), which shifted its distribution through time and, notably, exhibited a rapid range-  
22   wide decline at  $5280 \pm 180$  YBP. We consider how climate could have shaped this history by  
23   comparing fossil pollen records from eight New England sites with quantitative temperature and  
24   effective precipitation reconstructions and evaluating the realization of *Tsuga*'s climate niche  
25   through time. The comparisons indicate that multivariate climate change significantly influenced  
26   *Tsuga* abundance, including its abrupt decline and recovery. The comparisons show that the  
27   realized climate niche of *Tsuga* expressed today includes two important features that persisted  
28   through time. First, *Tsuga* pollen percentages reach their maxima (>30%) where July  
29   temperatures equal 18–20°C, but do so at two modes where annual precipitation equals either  
30   ~1100 or ~775 mm. The bimodality reflects *Tsuga*'s two geographic modes in the Great Lakes  
31   and Appalachian regions today, and explains past dynamics, such as short-lived peaks in *Tsuga*  
32   abundance associated with effective precipitation of ~775 mm at ca. 10,000 years before CE  
33   1950 (YBP). Second, the two peaks in *Tsuga* abundance follow negative correlations between  
34   temperature and precipitation such that the two modes shift toward high precipitation if  
35   temperatures are low (e.g., ~1400 and ~1000 mm at <18°C). Consequently, rapid cooling at  
36   5200±100 YBP facilitated widespread *Tsuga* declines because cooling did not coincide with  
37   increased precipitation. Abundance declined as local climates departed from optimal temperature  
38   and precipitation combinations. Recovery only followed as effective precipitation increased by  
39   >150 mm over the past 4000 years. A regionally calibrated model of the relationship of *Tsuga*  
40   pollen percentages to temperature and precipitation explains 70–75% of the variance in the

## Running head: Hemlock responses to Holocene climates

41 percentages at eight study sites. Iteratively excluding each site from the model shows that  
42 accurately representing the major features of the climate niche enables the model to predict the  
43 mid-Holocene decline and other past changes at the excluded site (site-level RMSE = 2.1-5.6%).  
44 Similar multivariate climate dynamics closely modulated the species' abundance throughout the  
45 Holocene with no evidence of additional large-scale disturbances.

46

47

48 **Key words:** climate change, climate niche, forests, New England, Holocene, hemlock

## Running head: Hemlock responses to Holocene climates

### 49 1. Introduction

50 Climate change, broad-scale disturbances, and other factors can alter the distributions of  
51 tree species in a variety of ways, but anticipating future change is difficult (Allen et al., 2010;  
52 Lenoir and Svenning, 2014). Useful precedents exist, however, in the Holocene history of  
53 eastern North American tree species such as *Tsuga canadensis* (L.) Carrière (eastern hemlock).  
54 Today populations of this shade-tolerant, long-lived canopy tree grow in dense stands on moist,  
55 acidic or rocky soils from the Great Lakes to the Appalachian Mountains (Foster, 2014)(Fig.  
56 1A). They can occupy multiple contrasting habitats on landscape scales (Kessell, 1979), and  
57 have different local adaptations to warm, dry versus cool, wet climates (Eickmeier et al., 1975).  
58 Such a negative trade-off between temperature and moisture may shape its distribution.  
59 Populations have expanded into new dry sites that were warm, as well as wet sites that were cool  
60 (Calcote, 2003). Populations appear limited by temperature in some areas (e.g., mountainsides in  
61 New Hampshire; Davis et al., 1980) and moisture in others (e.g., Michigan; Brubaker, 1975).  
62 Consequently, *Tsuga*'s history represents a model system for studying biogeographic responses  
63 to temperature and moisture changes, especially because the taxon's range, abundance, and  
64 association with other taxa changed continuously as climate changed since the last ice age  
65 (Davis, 1981; Davis et al., 1986; Graham and Grimm, 1990).

66 Fossil pollen records spanning >12,000 years indicates that the distribution of *Tsuga*  
67 shifted northward from the central Appalachians into the northeastern U.S. (hereafter "New  
68 England"), and then westward into the northern Great Lakes region (Davis et al., 1986; Webb III,  
69 1988; Parshall, 2002; Williams et al., 2004). The long-term geographic shifts have been widely  
70 attributed to climate changes (Fig. 1B, 2A-B)(e.g., Prentice et al., 1991; Shuman et al., 2002),  
71 but *Tsuga*'s abundance also declined precipitously across its range at ca. 5700-5000 calendar

## Running head: Hemlock responses to Holocene climates

72 years before CE 1950 (“YBP”) and remained low for many centuries to millennia before  
73 recovering in some regions (Davis, 1981; Allison et al., 1986; Bennett and Fuller, 2002). The  
74 decline played out within decades or less at some sites (Allison et al., 1986) and only rarely  
75 involved other taxa (Foster et al., 2006). Its association with climate change has not been clear.

76 In one eloquently articulated hypothesis, the rapid decline resulted from biotic  
77 interactions, such as a disease or insect outbreak, in the absence of synchronous rapid climatic  
78 change (Davis, 1981; Booth et al., 2012). The rapidity of the decline, the strong single-species  
79 dynamic, and evidence of forest insect outbreaks in a few locations at the time have provided  
80 enduring support for this hypothesis (Allison et al., 1986; Anderson et al., 1986; Bhiry and  
81 Filion, 1996). However, insect outbreaks did not affect all sites and other tree species with  
82 distinctly different ecologies also declined in some areas (Foster et al., 2006; Wang et al., 2015;  
83 Oswald et al., 2017). The primary alternative hypothesis links the decline to climatic change  
84 (Deevey, 1943; Yu et al., 1997; Haas and McAndrews, 1999; Foster et al., 2006; Shuman et al.,  
85 2009; Zhao et al., 2010). Drought has usually been regarded as the primary driver, but some  
86 evidence also points to a role for low temperatures (Calcote, 2003; Marsicek et al., 2013). Given  
87 the alternatives, the decline could represent an epiphenomenon initiated by one factor and then  
88 sustained by another (Booth et al., 2012).

89 Several enigmatic elements could hold the key to diagnosing the causes (Fig. 2). For  
90 example, low *Tsuga* abundance after the decline persisted as long as drought was sustained (e.g.,  
91 Booth et al., 2012; Marsicek et al., 2013), but effective precipitation (the net balance of  
92 precipitation and evapotranspiration) during the associated droughts was not as low as during  
93 earlier periods when *Tsuga* was highly abundant (Fig. 2B). Additionally, not all droughts  
94 associated with the decline began at the same time (Fig. 2B)(Newby et al., 2014), and in

## Running head: Hemlock responses to Holocene climates

95 Michigan specifically, *Tsuga* pollen percentages declined before drought intensified (Booth et  
96 al., 2012). Other unexplained aspects of the decline include why other taxa sometimes declined  
97 locally, but never across their entire ranges (Davis, 1981; Foster et al., 2006); why *Tsuga* did not  
98 shift towards a region with a more suitable climate (Shuman et al., 2009); and what caused an  
99 earlier peak and decline at ca. 9800 YBP in some areas (Zhao et al., 2010)(Fig. 2C).

100 Finally, the *Tsuga* decline can no longer be assumed to be either a widely synchronous  
101 event or the result of widespread rapid mortality as was originally suspected (Davis, 1981;  
102 Webb, 1982). Differences in both the timing and rate of decline have not been satisfactorily  
103 resolved, and some declines could represent a lack of regeneration and replacement rather than  
104 abrupt mortality (Fig. 2C). Differences exist even in records with limited temporal uncertainty  
105 and high sample density (see Liu et al., 2012), such as Spruce and Sutherland ponds in New  
106 York's Hudson Highlands (Maenza-Gmelch, 1997; Shuman et al., 2009)(Fig. 2C). The mean age  
107 of the decline in New England equals  $5280 \pm 180$  YBP (Shuman et al., 2009), but the decline at  
108 Spruce Pond dates to  $3800 \pm 100$  YBP (Maenza-Gmelch, 1997). These differences raise doubts  
109 about explanations such as rapidly spreading diseases or insect outbreaks.

110 Here, we evaluate the interactions of *Tsuga*'s multi-dimensional climate niche with the  
111 multivariate array of Holocene climate changes (Shuman and Marsicek, 2016). Environmental or  
112 Grinnelian niches often link the presence or absence of a taxon to factors such as climate  
113 (Peterson et al., 2011), but here, we focus on how abundance, represented by pollen, relates to  
114 climate. Non-linearities and multidimensionality within the niche could have produced counter-  
115 intuitive outcomes, especially when combined with the different independent trajectories of both  
116 temperature and moisture (Webb III, 1986; Crimmins et al., 2011)(Fig. 3). Changes may have  
117 played out via effects on physiological or ecological traits across different life history phases and

## Running head: Hemlock responses to Holocene climates

118 populations (e.g., Grubb, 1977; Webb III, 1986; Davis and Shaw, 2001). From a given starting  
119 point, either temperature or moisture can independently alter abundance (e.g., bold arrows, Fig.  
120 3A) and decreases or increases can arise where the opposite response might be expected if only  
121 one factor were considered (e.g., the hypothetical site trajectory in Fig. 3A where abundance  
122 reaches a minimum between period 1 and 2 at the model species' moisture optimum because  
123 temperature creates marginal conditions). Anticipating change is further complicated because the  
124 niche may not be fully realized at any given place in time or space (Gaston, 2003; Broennimann  
125 et al., 2007; Nogués-Bravo, 2009; Veloz et al., 2012; Maiorano et al., 2013).

126 We first describe the modern realized climate niche of *Tsuga* (pollen), and then discuss  
127 regional climate changes that would have interacted with *Tsuga*'s climate preferences during the  
128 Holocene. Using quantitative reconstructions of both summer temperatures and annual effective  
129 precipitation (Sachs, 2007; Newby et al., 2014), we reconstruct the past realization of the climate  
130 niche (the total climate envelope occupied at our study sites through time; Nogués-Bravo, 2009)  
131 and use a series of statistical models to evaluate the contribution of climate to the Holocene  
132 history of *Tsuga* in New England. Overall, we address two key questions: What is the structure  
133 of the realized climate niche of *Tsuga* through space and time? How well do climate changes  
134 predict the Holocene history of *Tsuga* abundance?

135

### 136 **2. Methods**

#### 137 Modern pollen & climate

138 To describe the modern relationships among climate variables and *Tsuga* pollen  
139 abundance, we use the North American modern pollen-climate dataset compiled by Whitmore et  
140 al. (2005) and described by Williams et al. (2006). We represent abundance as a percent of

## Running head: Hemlock responses to Holocene climates

141 terrestrial pollen, and focus on data from east of 105°W longitude. To evaluate the interaction of  
142 July temperatures and annual precipitation, we plot pollen data relative to each variable, but also  
143 consider abundance relative to the interaction among variables (Fig. 4). To do so, we calculate  
144 and then sum departures from the mean of both climate variables where *Tsuga* pollen exceeds  
145 1% (Fig. 4B-C). To do so, we first normalize the departures by the standard deviation of each  
146 respective variable. We also sub-divide the data into two sub-groups based on whether samples  
147 represent warm-moist (e.g., Appalachian) or cool-dry (e.g., Great Lakes) areas (Fig. 1A), which  
148 are associated with negative or positive departures from the climatic mean respectively (Fig. 4B).

149

### 150 Fossil pollen

151 We evaluate past *Tsuga*-climate relationships at eight representative sites in New  
152 England (Table 1). Four sites (Knob Hill, Little, Blood, and Deep ponds) form a north-south  
153 transect of detailed pollen records spanning from cool to warm areas of New England, while a  
154 second set of four sites (Guilder, Mohawk, Sutherland, and Spruce ponds) represents pairs of  
155 high and low elevation areas in the Berkshire and Hudson Highlands of Massachusetts and New  
156 York respectively. The elevational pairs also include unusual features of the *Tsuga* pollen record,  
157 including areas where *Tsuga* populations did not recover after the decline (like in many central  
158 Appalachian sites); where *Tsuga* populations experienced two declines (at ca. 10,000 and 5000  
159 YBP, such as at Sutherland Pond, NY, Fig. 2C); and where *Tsuga* populations declined much  
160 later than most other sites (at 3800 YBP at Spruce Pond, NY, Fig. 2C)(Gaudreau, 1986; Maenza-  
161 Gmelch, 1997). Overall, we analyzed four sites with high *Tsuga* pollen percentages (>20%) and  
162 four sites with low *Tsuga* pollen percentages (<10%). Data from most sites were generated at  
163 Harvard Forest using standard techniques (Foster et al., 2006; Oswald et al., 2007; Oswald et al.,

## Running head: Hemlock responses to Holocene climates

164 2018; Oswald and Foster, 2012), but data for Mohawk, Spruce, and Sutherland ponds (Gaudreau,  
165 1986; Maenza-Gmelch, 1997) were obtained from the Neotoma Paleoecology Database  
166 (Williams et al., 2018).

167

### 168 Climate reconstructions

169 We compare the fossil pollen data with quantitative temperature and effective  
170 precipitation estimates based on alkenone paleothermometry (Brassell et al., 1986; Sachs, 2007)  
171 and lake-level reconstructions (Marsicek et al., 2013; Pribyl and Shuman, 2014). These estimates  
172 derive from four locations (Fig. 1, 2): temperatures from cores collected off the coasts of Nova  
173 Scotia (GGC30) and Virginia (GGC19)(Sachs 2007) and effective annual precipitation from  
174 Davis and Deep ponds in western and eastern Massachusetts respectively (Newby et al., 2011;  
175 Marsicek et al., 2013; Newby et al., 2014). Continental temperature records are rare and difficult  
176 to obtain, but in New England, we make the assumption that regional temperature changes  
177 influenced both terrestrial and marine locations. Historically, mean annual temperatures onshore  
178 and sea-surface temperatures (SSTs) in the region correlate. Climate division data from across  
179 Massachusetts (Vose et al., 2014) for CE 1948-2016 correlate ( $r = 0.69$ ) with SSTs from 42-44°  
180 N and 65-70° W (Kaplan et al., 1998); both datasets show a period of low temperatures after the  
181 warm CE 1950s and a subsequent warming trend with similar inter-annual variability.  
182 Temperature and effective precipitation time series for the Holocene also share significantly (and  
183 negatively) correlated signals at millennial to multi-century timescales despite deriving from  
184 independent data sources, which provides confidence that they represent a coordinated set of  
185 climate changes around New England (Shuman and Marsicek, 2016). Appendix I describes the  
186 specific records, their age control, and the interpolation and analytical methods.

## Running head: Hemlock responses to Holocene climates

187 We linearly interpolated the reconstructed climate anomalies to the locations of our  
188 pollen records based on latitude and longitude. Absolute temperature and precipitation time  
189 series for each fossil pollen record were then derived by combining the interpolated paleoclimate  
190 anomalies with the mean July temperatures and annual precipitation rates for CE 1941-1970 for  
191 each location from the 800-m resolution PRISM time-series climate dataset (Daly et al., 2008).  
192 The absolute temperature and precipitation time series, thus, account for differences related to  
193 factors such as elevation and latitude, and are important for evaluating the climate niche (Fig. 3).  
194

### 195 *Reconstructing past climate-abundance relationships*

196 Ancient changes in the realization of species' climate niches have been evaluated using  
197 fossil data in combination with climate model simulations (Nogués-Bravo, 2009; Veloz et al.,  
198 2012; Maiorano et al., 2013). Here, we interpolate the paleoclimate reconstructions as the basis  
199 for our statistical model because we want to capture the specific sequence of both forced and  
200 stochastic climate variations at sub-millennial scales (Fig. 2). To match the fossil pollen  
201 percentages to the full Holocene array of mean July temperatures and annual effective  
202 precipitation for each site, we also interpolate the data in time. We use uniform 50-yr time steps  
203 to ensure that the major patterns in the original data were not aliased.

204 We compare current and past relationships among *Tsuga* pollen percentages, mean July  
205 temperature, and mean annual precipitation by randomly pairing modern and fossil pollen  
206 percentages from locations and times with the same climates. To do so, we subdivide all of the  
207 data into 0.5°C and 50 mm moving windows regardless of time, and compare up to 1000 random  
208 pairs per window containing at least one fossil sample and a non-zero modern median percentage  
209 (i.e., where the two realized niches overlap and are well constrained by data). In each window, if

## Running head: Hemlock responses to Holocene climates

210 the 95% distribution of the random differences did not include zero, we infer a significant  
211 difference.

212

### 213 Models of past pollen percentages

214 Finally, we apply generalized additive models (GAMs), which are locally weighted  
215 polynomials, to estimate how well mean July temperature and annual effective precipitation data  
216 explain the time series of pollen percentages. GAMs can account for the non-linearities in the  
217 climate-abundance relationships (Wood, 2006a). They do not fit a specific global function (e.g.,  
218 linear, quadratic) to the complex relationships, but instead, use local smoothing in the  
219 reconstructed paleoclimate space (e.g. locally-weighted scatterplot smoothing or lowess;  
220 Cleveland, 1979). Our models use tensor product smooths to incorporate the interactive  
221 temperature and effective precipitation effects (Wood, 2006b). They sub-divide climate space  
222 and apply the local, non-parametric polynomials within each window in a fashion that ensures no  
223 sharp breaks in the climate-pollen relationships between windows (Wood, 2006a).

224 We apply the GAMs to sites individually and to the entire dataset with each site withheld  
225 iteratively for model validation. The single site (“site-specific”) models provide an estimate of  
226 how well the relative sequence of temperature and moisture changes explain the local variations  
227 in *Tsuga* pollen percentages. Because of the non-linear relationships involved, we use the GAMs  
228 in place of linear regression to measure the variance explained. We test their significance by  
229 comparing the site-specific models with a null distribution of models for each site that use only  
230 randomly generated time series with the same autoregressive characteristics as the paleoclimate  
231 reconstructions (Appendix I). If the GAMs fit the *Tsuga* pollen percentages only because of the  
232 flexibility of the GAM or the ability of similarly smoothed time series to produce spurious

## Running head: Hemlock responses to Holocene climates

233 correlations (Granger and Newbold, 1974), the variance explained by the site-specific GAM  
234 would not exceed the range of variance that could be explained by autoregressive models alone  
235 (Telford and Birks, 2011).

236 The regional (“leave-one-out”) models test the relationships between *Tsuga* pollen  
237 percentages and the absolute climates rather than the relative sequence of climate changes. By  
238 iteratively excluding each site, we test the hypothesis that a broad sampling of *Tsuga*’s climate  
239 niche across time and space provides sufficient information to predict the species’ history.  
240 Because data representing multiple locations and times were required to fully sample the  
241 Holocene environmental space, the exclusion of some sites from under-sampled climate regions  
242 produced deficient models. Models excluding these sites were inadequate to test the hypothesis,  
243 but reveal characteristics of the climate niche essential for accurate prediction.

244 To create each regional model iteration, we used a generalized additive mixed model that  
245 combines a GAM with a linear mixed-effect model to treat the individual locations (sites) as  
246 random effects (Wood, 2006a). For each site excluded during model construction, the regional  
247 mixed-effect model included only the climate data and pollen percentages from the most recent  
248 sample to account for the random effects when predicting change earlier in the Holocene. None  
249 of the models rely on any modern calibration data, but rather determine the best fit among the  
250 paleoclimate and *Tsuga* time series either for each site individually or for the full set of  
251 calibration sites using data for all time intervals >550 BP. All of the pollen percentages were  
252 exponentially transformed by 0.25 before applying the GAM function in R (R Core Team, 2017).  
253 To further ensure that the models were not overfit, we minimized the flexibility of the smoother  
254 by restricting the maximum number of basis functions, k, for each model: 5 for site-specific  
255 models and 10 for the regional “leave-one-out” models, which incorporated more data. Doing so

## Running head: Hemlock responses to Holocene climates

256 substantially reduced the degrees of freedom in the model and is conservative relative to the  
257 recommended values of k, which are  $10n^{2/9}$  where n is the number of data (Kim and Gu 2004);  
258 the recommended values for our site-specific and regional models are 33 and 51 respectively.

259 Furthermore, we examined a multivariate climate signal akin to using sums of growing-  
260 degree days and soil moisture to predict productivity increases (Woodward, 1987; Prentice et al.,  
261 1992). Starting from the cool, dry early Holocene when *Tsuga* abundance first rose, increases in  
262 either temperature or moisture could have increased abundance (e.g., perpendicular bold arrows,  
263 Fig. 3A). To represent this heuristic climate signal, we summed the positive deviations of  
264 temperature and effective precipitation from a baseline determined by the Holocene mean at each  
265 site. The paleoclimate data were normalized to z-scores (departures from the Holocene mean in  
266 standard deviation units) and then the positive values were combined into a single time series. As  
267 long as at least one variable has a positive value, *Tsuga* abundance was predicted to be above  
268 zero (such as would be the case for either perpendicular bold arrow in Fig. 3A). We do so to  
269 further ensure that the GAM fits represent meaningful signals in the climate data rather than  
270 spurious non-linear fits. The R code and data used are provided as a Supplement to this paper.  
271

### 272 **3. The realized climate niche of *Tsuga canadensis* today**

273 *Tsuga* pollen represents nearly 50% of the terrestrial pollen sum in areas with mean July  
274 temperatures of about 20°C and annual precipitation above 775 mm (Fig. 4). With respect to July  
275 temperatures, *Tsuga* pollen percentages have a unimodal and nearly symmetric distribution about  
276 a mean of 19.2°C with a standard deviation of 1.2°C (Fig. 4A). Distributions with respect to  
277 temperature are similar in both wet and dry areas (orange lines, Fig. 4A). The relationship with  
278 annual precipitation has two modes: one narrow mode near the sharp lower limit of *Tsuga* pollen

## Running head: Hemlock responses to Holocene climates

percentages >1% at 775 mm and a second broad mode centered around a mean of 1106 mm (Fig. 4D). These modes correspond to peak abundances in the Great Lake region (gray symbols in Figures 1A and 4D) and Appalachian Mountains (green symbols in Figures 1A and 4D) respectively. Between the two modes at 900 mm, the percentages only achieve a maximum of ~10% as shown by local-weighted means of the percentages with respect to precipitation (orange lines, Fig. 4D).

The two modes become more pronounced when viewed along the axis of temperature-precipitation interaction (Fig. 4B). Percentages rise to two distinct peaks of >25%: one about 1 standard deviation below the mean (cool, dry areas; negative departures from the means) and one about 1 standard deviation above the mean (warm, moist areas; positive departures from the means). When we split the data along this axis into negative and positive groups, and plot the data in bivariate temperature versus precipitation space (Fig. 4C), we observe that *Tsuga* pollen percentages increase along two parallel ridges of abundance with one representing drier and cooler sites than the other. The two groups also tend to split out geographically: the negative group predominantly corresponds to the mode of abundance in the Great Lakes region and the positive group to the Appalachian-New England mode (Fig. 1A).

In both groups, maximum abundance tracks a negative correlation between mean July temperatures and annual precipitation (Fig. 4C). Linear regression reveals that the negative group follows a line with a slope of -84.6 mm/°C and an intercept of 2480 mm ( $R^2=0.66$ ;  $n=1434$ ); the positive group has a slope of -62.1 mm/°C and an intercept of 2340 mm ( $R^2=0.24$ ;  $n=923$ ). Consequently, about 140 mm of annual precipitation separates the two groups, but they come close to merging together in wet and cool areas. Data gaps, which make the groups visually distinct in Fig. 4C, represent the area of the Great Lakes themselves, but low *Tsuga* pollen

## Running head: Hemlock responses to Holocene climates

302 percentages in the trough between the groups represents the absence of extensive *Tsuga*  
303 populations in western Ohio, Indiana, southern Michigan, and other areas between the arms of  
304 the species distributions in Appalachia and the northern Great Lakes region (Fig. 1). Low  
305 abundance in this region is not a function of historic land clearance, but has persisted since  
306 before European settlement (Shane, 1991; Clark et al., 1996; Wang et al., 2015; Paciorek et al.,  
307 2016; Goring et al., 2016).

308

### 309 **4. Climate, *Tsuga* abundance, and the climate niche through time**

#### 310 *4.1 Climate trajectories*

311 *Tsuga* populations in New England have experienced multiple changes in the  
312 combination of temperature and precipitation over the Holocene, which are equivalent to  
313 travelling from Minnesota to New England today (as characterized by the climate history at  
314 Blood Pond in Fig. 1B). Early in the Holocene, both mean July temperatures and total annual  
315 effective precipitation increased substantially (by ~2-3°C in Fig. 2A and >300 mm in Fig. 2B),  
316 but after ca. 7000-5000 YBP, a long-term trade-off between temperature and effective  
317 precipitation shaped the regional history. July temperatures declined by ~1°C, but effective  
318 precipitation increased by an additional ~300 mm (Fig. 2A-B). Similar trends also affected the  
319 western portion of *Tsuga*'s range (Calcote, 2003). Because the effective precipitation changes  
320 were large, populations tracking their optimal climate conditions would have had to move  
321 westward more than northward. Climates once found in central Massachusetts now exist in  
322 Minnesota, Wisconsin, Michigan, and western New York (Fig. 1B).

323 In addition to the long trends, paleoclimate time series also show evidence of 1) abrupt  
324 cooling episodes, notably by >1°C at 5400 (5650-5300) YBP in the region of the Labrador

## Running head: Hemlock responses to Holocene climates

325 Current (GGC30 in Fig. 2A), and 2) multi-century droughts recorded at both inland and coastal  
326 areas at 4200–3900, 2900–2100, and 1300–1200 YBP (Fig. 2B). Some changes were spatially  
327 heterogeneous, such as at 5800 YBP when water levels fell at the western lake-level site, Davis  
328 Pond, but rose at the eastern lake-level site, Deep Pond (Fig. 2B)(Newby et al., 2014; Shuman  
329 and Burrell 2017).

330 The changes were ecologically large. They equal differences among biomes today.

331 Increases in temperature and precipitation after 12,000 YBP compare to moving today from  
332 boreal forests in northern Minnesota down through forests with *Tsuga* populations in Wisconsin  
333 and Michigan (blue symbols, Fig. 1B). Rapid summer cooling after ca. 5700 YBP was then  
334 analogous to shifting eastward to the lowlands of western New York and southern Ontario, or in  
335 some cases, coastal southern New England, where *Tsuga* pollen percentages have been low since  
336 before European settlement (orange, Fig. 1B). Finally, additional cooling and an increase in  
337 effective moisture by 3200 YBP (Fig. 2) equaled moving into the New England highlands where  
338 *Tsuga* pollen percentages are high today (black, Fig. 1B).

339 The climate trajectory of each site thus passed through unique combinations of absolute  
340 temperature and precipitation with almost no repetition of earlier combinations (Fig. 5A).

341 Climates of the early Holocene did not overlap with those of more recent millennia (e.g.,  
342 compare colored symbols representing early-, middle-, and late-portions of the Holocene, Fig.  
343 1B). The differences prevent the early *Tsuga*-climate relationship at any given site from being  
344 used to predict later abundance at that site and vice versa. Data from the whole environmental  
345 space are required.

346 The individual sites followed nearly parallel trajectories through different portions of the  
347 modern climate niche (Fig. 5A). Each site began the Holocene where effective annual

## Running head: Hemlock responses to Holocene climates

348 precipitation was too low for *Tsuga* (like Minnesota today). As temperatures and effective  
349 precipitation increased, the sites then moved upward to the right in Fig. 5A and into the area of  
350 climate space occupied by *Tsuga* today. Some sites then remained within the climate space  
351 represented by the negative (Great Lakes) group of modern *Tsuga* samples (e.g., the trajectory at  
352 Knob Hill Pond, black line in Fig. 5A), but others crossed into the space occupied by the positive  
353 Appalachian group (e.g., at Blood Pond, brown line in Fig. 5A) or remained at the margins (e.g.,  
354 Spruce Pond, red line in Fig. 5A).

355 After ca. 7000 YBP, the locations in climate space shifted up to the left in Fig. 5A  
356 because temperatures decreased as effective precipitation increased. The mean slope of the  
357 temperature-precipitation correlation after ca. 7000 YBP equaled -97.5 mm/°C, and ensured that  
358 *Tsuga*-dominated sites tracked within the ridges of *Tsuga* abundance (e.g., Knob Hill and Blood  
359 ponds, black and brown lines in Fig. 5A respectively). When temperatures declined by 5400  
360 YBP (Fig. 2A), however, climate trajectories shifted down to the left in Fig. 5A (bold lines) and  
361 cut across rather than along the ridges of sustained *Tsuga* abundance. At this one time in the past  
362 7000 YBP, the climate trajectories for the sites with abundant *Tsuga* moved out of the optimal  
363 climate space for high *Tsuga* pollen percentages (Fig. 5A). The addition of a third variable, such  
364 as winter temperature, could have shifted the conditions even further from *Tsuga*'s optima, but  
365 we lack suitable data to evaluate this possibility.

366

### 4.2 Niche realizations through time and space

368 Combining the paleoclimate trajectories inferred from the lake-level and alkenone  
369 records with the observed pollen percentages at our eight sites provides a Holocene perspective  
370 on the realized climate niche (Fig. 5-6). From this perspective, *Tsuga* pollen percentages also

## Running head: Hemlock responses to Holocene climates

371 express two parallel maxima in climate space with negative temperature-precipitation  
372 correlations (green symbols, Fig. 5B). The reconstructed Holocene niche occupied some warmer  
373 and drier climates than the modern niche (compare green versus black symbols in Fig. 5B), and  
374 where the two realizations of the niche overlap, fossil percentages were significantly greater than  
375 those today in 28 of 85 individual windows in climate space (32.9% of cells in Fig. 5C). Overall,  
376 however, the 95% distribution of all modern-minus-fossil sample differences (10.0 to -24.6  
377 percentage points; median: -4.0 percentage points) includes zero and is consistent with many  
378 differences deriving from stochastic processes and reconstruction uncertainties (Fig. 5D).

379 Over time, the pollen percentages increased or declined in a manner consistent with the  
380 bimodality observed in the climate niche today (Fig. 6; Supplementary Animation). The  
381 independence of the modern and paleoecological datasets required no alignment of past and  
382 modern patterns, particularly early in the Holocene (>9000 YBP, black highlighted symbols in  
383 Fig. 6). However, our study sites followed bimodal trajectories within the climate-abundance  
384 space delineated by modern data (gray in Fig. 6) and reached two maxima like those observed  
385 today: one in association with cool, dry climates (negative departures from mean conditions, Fig.  
386 6) and one with warm, moist climates (positive departures from mean conditions, Fig. 6). All  
387 sites experienced minima in abundance when their local climate neared the mean climate of the  
388 distribution (zero in Fig. 6).

389 The trajectories of sites with high percentages tracked within the two modern modes  
390 (e.g., Blood and Knob Hill ponds, Fig. 5-6) whereas those with low percentages followed the  
391 margins (e.g., Spruce Pond, Fig. 5-6). The amplitudes of change typically declined as sites  
392 represented increasingly marginal climates for *Tsuga* (Fig. 6H). As a result, sites like Spruce and  
393 Sutherland ponds (Fig. 6C-D) followed bimodal trajectories with low maxima (<10%) about 1-2

## Running head: Hemlock responses to Holocene climates

394 sd from the mean combination of temperature and precipitation, whereas sites like Guilder and  
395 Little ponds reached high maxima (>15%) at 0.5-1 sd from the mean (Fig. 6A-B). Knob Hill  
396 Pond in cool, dry Vermont did not follow a bimodal trajectory, but remained entirely within the  
397 climate space occupied by the modern negative (cool, dry Great Lakes) mode (Fig. 6E).

398         The bimodality in climate space corresponds to peaks in *Tsuga* pollen time series. For  
399 example, when *Tsuga* pollen percentages first increased in New England before 9000 YBP, only  
400 the negative (cool, dry Great Lakes) mode of the modern distribution was well represented  
401 (black circles in Fig. 6; see also the early frames of the Supplementary Animation). These early  
402 samples form the earliest peaks in *Tsuga* pollen percentages, like those at Sutherland and Spruce  
403 ponds (Fig. 2C)(Maenza-Gmelch, 1997) and elsewhere in the mid-Atlantic region (Zhao et al.,  
404 2010). Because the different sites experienced the optimal absolute conditions for peak  
405 percentages at different times (e.g., at different latitudes and elevations), the early peaks differ  
406 modestly in time (compare black filled versus open circles for >10,500 YBP and 10,500-9000  
407 YBP respectively at sites like Sutherland and Guilder ponds in Fig. 6; see also Fig. 2C).

408         Low *Tsuga* pollen percentages then followed from ca. 9000-8000 YBP as most sites  
409 moved climatically between the modes of the niche (and the youngest black circles plot near zero  
410 along the x-axis in Fig. 6). At the same time, however, *Tsuga* pollen percentages first increased  
411 at our coldest and driest site, Knob Hill Pond, which did not experience an early peak in  
412 abundance (Fig. 2B) and never experienced the climate associated with the modern positive  
413 mode (Fig. 6E; black symbols in the Supplementary Animation).

414         After 8000 YBP, new combinations of temperature and precipitation coincided with  
415 renewed increases in *Tsuga* pollen percentages. The changes established the positive (warm,  
416 moist) mode in New England where it remains today (positive x-axis values in Fig. 6). When

## Running head: Hemlock responses to Holocene climates

417 *Tsuga* pollen percentages declined at most sites by ca. 5200 YBP (black crosses in Fig. 6),  
418 conditions usually shifted away from each site's local optimum and back towards the local intra-  
419 mode minimum, close to earlier minimum samples from 9000-8000 YBP (compare black circles  
420 and crosses in Fig. 6). High percentage samples at Guilder and Little ponds at  $x = 0$  (i.e., above  
421 the black crosses in Fig. 6A-B) represent the transient values of the decline itself, which aligns  
422 with the intra-mode minimum (Supplementary Animation). After the decline, bimodality  
423 remained with peaks in abundance represented by Little, Guilder, and Spruce ponds (crosses in  
424 Fig. 6H). As effective precipitation increased after ca. 3700 YBP, the sites re-occupied optimal  
425 climates and *Tsuga* pollen percentages correspondingly increased again.  
426

## 427 **5. Statistical models of *Tsuga* pollen percentages**

### 428 5.1 Climate signals

429 The similarities between modern and past *Tsuga*-climate relationships (Fig. 5-6) could  
430 only emerge from persistent and robust associations among the paleoclimate and pollen time  
431 series. In fact, the sum of the positive anomalies in the alkenone temperature and lake-based  
432 effective precipitation reconstructions (normalized as z-scores) indicate that the sequence of  
433 climate changes would have repeatedly favored high *Tsuga* abundance (Fig. 7). The signal  
434 includes a sharp rise to peak favorability by 8200 YBP, an abrupt mid-Holocene decline in  
435 favorable conditions, a minimum from ca. 5000-4000 YBP, and then a progressive rise in  
436 favorability over the last four millennia (e.g., representative examples from Deep and Knob Hill  
437 ponds, Fig. 7). Key local details are also similar including short-lived maxima in both the climate  
438 signal and *Tsuga* pollen percentages between droughts at Deep Pond at 4350, 3000, and after  
439 1600 YBP (Fig. 7A) and a short-lived minimum associated with cooling at 6250 YBP at Knob

## Running head: Hemlock responses to Holocene climates

440 Hill (Fig. 7B). Notably, the sharp mid-Holocene declines in the climate-derived time series have  
441 different median ages (5150 YBP at Deep Pond and 5550 YBP at Knob Hill), which parallel the  
442 observed difference in the median ages of the local *Tsuga* declines: 5150 YBP at Deep Pond and  
443 5500 YBP at Knob Hill. An important area of mismatch relates to differences before ca. 8500  
444 YBP (possibly because this heuristic approach would not account for bimodality in the niche).  
445 Based on the coherency of these climate signal models and the fossil pollen data, we proceeded  
446 to develop GAMs to quantify the relationships.

447

### 448 5.2 Generalized additive models of *Tsuga* abundance

449 GAMs based on the site-specific estimates of mean July temperatures and annual  
450 effective precipitation explain the majority of the variance in the *Tsuga* pollen time series (mean  
451 adjusted  $R^2 = 0.60$ ; range = 0.29-0.85; Table 2). Root mean squared errors (RMSE) varied from  
452 0.9-5.2 percentage points (Fig. 8-9), and equal 12-15% of the local maxima in *Tsuga* pollen  
453 percentages (Table 2). The variance explained ranges from 69% to 85% at sites with high *Tsuga*  
454 (>20%) pollen percentages (Guilder, Knob Hill, Little, and Mohawk ponds), and from 29% to  
455 54% at the low abundance sites (Blood, Deep, Spruce, and Sutherland). The variance explained  
456 by the GAMs based on the climate reconstructions is significant. It consistently exceeds the 95%  
457 range of variance explained by auto-correlated random time series (Fig. 10, Table 2). The null  
458 distributions show the potential spurious explanatory power arising from autocorrelated predictor  
459 variables and a flexible GAM, but models based on the actual paleoclimate reconstructions have  
460 more explanatory power than expected from these factors alone (Fig. 10).

461 The regional “leave-one-out” models consistently fit 70-75% of the variance in the data  
462 used to develop each model (Table 2). Five models are sufficiently complete that they do not

## Running head: Hemlock responses to Holocene climates

463 differ meaningfully from each other (right panels, Figs. 8 & 9D) or from the complete dataset  
464 (Fig. 5B), but three deficient models do not fully represent the Holocene climate space or the  
465 details of the *Tsuga*-climate relationship (right panels, Fig. 9A-C). Overall, correlation between  
466 predicted and observed pollen percentages at sites predicted using complete models ranges from  
467 0.23 to 0.65, but those for incomplete models are <0.23 (Table 2). All of the complete models  
468 accurately predict a mid-Holocene decline (Fig. 8).

469 The five complete models individually exclude Blood, Mohawk, Deep, Sutherland, and  
470 Spruce ponds. The first three experienced paleoclimates that followed trajectories through well-  
471 constrained portions of the model (right panels, Fig. 8A-C), whereas Sutherland and Spruce  
472 ponds lie along the margin (Figs. 8D & 9D). In each model, the *Tsuga*-climate relationship is  
473 bimodal with the maxima in the pollen percentages expressing negative temperature-moisture  
474 correlations as described for modern data (dark green in right panels, Fig. 8). Limited constraints  
475 on the random site effects (e.g., soils) cause the predicted and observed mean percentages to  
476 differ (orange and green lines in left panels, Fig. 8), but the models accurately predict important  
477 features of the pollen percentages at each excluded site including the mid- and late-Holocene  
478 maxima and the abrupt mid-Holocene decline. They also accurately represent additional short-  
479 lived fluctuations at ca. 4300 and 3000 YBP at Deep Pond (orange lines, left panels, Fig. 8).

480 Other details are poorly predicted, including the early Holocene maximum at Sutherland  
481 Pond (orange line, left panel Fig. 8D). The Spruce Pond model represents the late decline there  
482 after ca. 3500 YBP and includes early and mid-Holocene maxima, but the *Tsuga* pollen  
483 percentages are commonly over-predicted and an inaccurate second decline is predicted after ca.  
484 2000 YBP (orange line, left panel Fig. 9D). Although the data from Spruce Pond inform the  
485 relevant region along the margin of the Sutherland Pond model and vice versa (note the similar

## Running head: Hemlock responses to Holocene climates

486 trajectories in Figs. 8D & 9D), the models correctly predict large differences in the timing of the  
487 decline at the two sites. Otherwise, the predictions for Sutherland are more accurate than for  
488 Spruce, especially after 8000 YBP.

489 The deficient models target three high abundance sites, Knob Hill, Guilder, and Little  
490 ponds (Fig. 9A-C). They predict some commonly observed features such as early-Holocene  
491 peaks in *Tsuga* pollen percentages, but fail to produce the mid-Holocene decline and do not fully  
492 represent the bimodal structure of the *Tsuga*-climate relationship. At Knob Hill Pond, the  
493 reconstructed climate at the time of the decline lies outside of the well-constrained model space  
494 (blue line in right panel, Fig. 9A) and, consequently, no decline is predicted (orange line in left  
495 panel, Fig. 9A). At Guilder Pond, the regional model is similarly incomplete (blue line in right  
496 panel, Fig. 9B); the model produces a rapid shift in *Tsuga* abundance in the mid-Holocene, but in  
497 the wrong direction (Fig. 9B). The regional model for Little Pond insufficiently represents the  
498 minimum between modes in *Tsuga* pollen percentages and contains a plateau of high abundance  
499 with no clear bimodality (right panel, Fig. 9C); the oversimplified model prohibits the prediction  
500 from declining to a minimum (orange line in right panel, Fig. 9C). In the raw climate-abundance  
501 relationships for both Guilder and Little ponds, however, low percentages immediately after the  
502 decline align with the intra-mode minimum in the modern climate niche (black crosses, Fig. 6A-  
503 B). These GAMs fail, but they should be expected to fail. They are incomplete or inaccurate  
504 representations of the climate niche.

505

## 506 **6. Discussion**

### 507 6.1 A complex climate niche

## Running head: Hemlock responses to Holocene climates

508        *Tsuga*'s realized climate niche has two distinctive features, which appear to have existed  
509 throughout the Holocene: bimodality and a negative correlation between temperature and  
510 precipitation (Fig. 4-6). At any given point in time, our few samples from New England may not  
511 fully realize or may misrepresent through under-sampling (alias) structure within the niche  
512 (Supplementary Animation), but by sampling across the full range of Holocene climates  
513 represented across space and through time, we obtain a more complete view of fundamental or  
514 conservative aspects of the niche than otherwise possible. When the full trajectories of the  
515 individual sites are evaluated, the bimodality (Fig. 6) and negative temperature-precipitation  
516 correlation apparent today (Fig. 5B) remain despite our Holocene analysis excluding samples  
517 from <550 YBP. When models represent these major features of the climate niche, they  
518 accurately reproduce the Holocene history of *Tsuga* (Fig. 8) despite the many potential sources  
519 of analytical error such as climate reconstruction and age uncertainties, extrapolation of climate  
520 anomalies from a few sites to a region, and poorly constrained site effects. When models do not  
521 resolve the major structures of the niche, they fail to reproduce the history (Fig. 9).

522        The two persistent elements of the niche must represent interactions among many  
523 processes. For example, *Tsuga* germination peaks at 12-17°C with significant limitations below  
524 6°C or above 21°C (Stearns and Olson, 1958; Olson et al., 1959), but drought within the first  
525 several years after germination can cause seedling mortality of >80% (Goerlich and Nyland,  
526 2000). At *Tsuga*'s western range limit, sites show a trade off between temperature and  
527 precipitation (one high if the other is low) in association with initial *Tsuga* establishment  
528 (Calcote, 2003). Thus, both temperature and moisture availability may interact with *Tsuga*'s  
529 distribution in multiple ways from the level of seeds to metapopulations to structure the realized  
530 climate niche. Other factors, such as biotic interactions (Rooney et al., 2000; Krueger and

## Running head: Hemlock responses to Holocene climates

531 Peterson, 2006; Witt and Webster, 2010), correlations among the genetic bases of key traits  
532 (Etterson and Shaw, 2001), and correlations among important climate variables (Veloz et al.,  
533 2012) probably also contribute to this structure.

534 The regional bimodality with respect to climate does not appear, however, to represent  
535 factors like land use or taphonomy (e.g., pollen percentage effects). The minimum in abundance  
536 between modes exists across portions of southern Michigan, Indiana, Ohio, western New York,  
537 and Ontario, which have not historically supported many *Tsuga* populations; large *Tsuga*  
538 populations were not removed by Euro-American forest clearance (Shane, 1991; Clark et al.,  
539 1996; Wang et al., 2015; Paciorek et al., 2016; Goring et al., 2016). Likewise, high abundance of  
540 other pollen types did not artificially suppress the pollen signal of *Tsuga*, which was inherently  
541 low in this region. Instead, bimodality exists because more than one combination of climate  
542 conditions appears to favor high abundance. The multiple combinations of dynamics involved,  
543 possibly including its ability to simultaneously compete successfully against deciduous tree taxa  
544 under different edaphic extremes at landscape scales (Kessell, 1979), could favor high abundance  
545 for different reasons in more than one region.

546 Additionally, different genotypes could play a role in the bimodality if they are adapted  
547 to different climates (Davis and Shaw, 2001). A higher frequency of unique alleles in  
548 Midwestern than Appalachian populations could hint at different local adaptations (Potter et al.,  
549 2012). However, chloroplast DNA differentiation from the main range to outlying populations  
550 appears modest (Wang et al., 1997) and the available genetic data indicate similar ancestries of  
551 Midwestern and New England populations (Potter et al., 2012).

552 Local adaptations in *Tsuga* populations are clear, however, and include differences in the  
553 optimal temperatures for germination across geographic regions (Stearns and Olson, 1958) and

## Running head: Hemlock responses to Holocene climates

554 in seedling carbon fixation rates and water-use efficiency (Eickmeier et al., 1975). The later is  
555 relevant to the negative temperature-moisture correlation within the niche because moisture  
556 stress substantially inhibited carbon fixation in cool-adapted seedlings from northern Wisconsin  
557 compared to warm-adapted seedlings from southern Wisconsin. The seedlings associated with  
558 warm southern areas retained 52% of their photosynthetic capacity under drought stress  
559 compared to only 29% for those from cool northern areas (Eickmeier et al., 1975). Further  
560 analyses are required, but these observations indicate that physiology and population genetics  
561 may underlie our finding that *Tsuga* only flourished under cool climates if moisture availability  
562 was high and warm climates if moisture availability is low (Fig. 4).

563 The Holocene niche differs in some respects from the one realized today (Fig. 5B-C).  
564 Historic land use could well explain why fossil pollen percentages exceeded modern values in  
565 32.9% of the climate space (Fig. 5C)(Fuller et al., 1998; Goring and Williams, 2017). Additional  
566 factors, such as a potentially more mild seasonal range in early Holocene New England than in  
567 continental Minnesota today, must have also alleviated some current limitations to broaden the  
568 niche into warm, dry climates where *Tsuga* does not currently grow (Xs in Fig. 5C). Even with  
569 these differences, and considering the various reconstruction uncertainties, the complex  
570 Holocene niche depicted by our dataset conforms closely to the one expressed today (Fig. 5-6).  
571

### 572 6.2 The role of Holocene climate change

573 The stability of key aspects of the climate niche through time has an important corollary:  
574 the reconstructed Holocene climate changes explain the major features of *Tsuga*'s history over  
575 the past 12,000 years. If not, the key features of the realized climate niche would not have been  
576 stable (Lenoir and Svenning, 2014).

## Running head: Hemlock responses to Holocene climates

577 Several lines of evidence conform to the hypothesis that the major changes in *Tsuga*'s  
578 abundance derived from the interactions of independent trajectories of temperature and moisture  
579 with a multidimensional climate niche (Fig. 3)(Webb III, 1986; Prentice et al., 1991). First, the  
580 independent modern and Holocene climate-abundance relationships are similar (Fig. 5-6).  
581 Second, heuristic models (Fig. 7) and site-specific GAMs explain a majority of the variance in  
582 *Tsuga* pollen percentages (scatter plots & black lines in Fig. 8-9; Table 2), and the *Tsuga*-climate  
583 relationships are stronger than null models would have anticipated (Fig. 10). Finally, complete  
584 "leave-one-out" GAMs, while imperfect, predict major features of *Tsuga*'s history at the  
585 validation sites, including the mid-Holocene decline (orange lines, Fig. 8).

586 Davis (1981) ruled out climate as a driver of the *Tsuga* decline, in part, because of a lack  
587 of evidence for mid-Holocene climate changes, but such evidence is no longer lacking. The  
588 decline emerges as a clear part of the Holocene climate record (Fig. 7), which vegetation history  
589 in the region typically tracked (Shuman et al., 2004; 2009; Williams et al., 2002). At finer  
590 temporal and spatial scales than considered here, disturbance agents such as forest defoliators  
591 may have locally facilitated the mid-Holocene decline (Anderson et al., 1986; Bhiry and Filion,  
592 1996), but the first-order importance of disturbance would represent an unusual, and undetected,  
593 exception to persistent regional climate-vegetation relationships (Shuman et al., 2019).

594 All of the heuristic, site-specific, and complete regional "leave-one-out" models predict  
595 abrupt, mid-Holocene declines (Fig. 7-8). Even considering the deficient models (Fig. 9),  
596 climate-induced declines should have been common. Furthermore, evidence of insect outbreaks  
597 has rarely been found even in locations where they may have been favorably preserved (Oswald  
598 et al., 2017) and broadleaf tree taxa susceptible to different diseases and parasites declined  
599 synchronously with *Tsuga* in some ecosystems (Foster et al., 2006; Wang et al., 2015). Because

## Running head: Hemlock responses to Holocene climates

600 the *Tsuga* decline occurred at different times in different places with different absolute climates,  
601 the potential role of a single biotic factor that co-varied with climate is also limited (Fig. 8-9).  
602 Climate-pollen relationships also did not change during the decline like they did after large  
603 disturbances in other conifer-dominated ecosystems (e.g., Calder and Shuman, 2017); model  
604 errors here are not systematically correlated with any specific dynamics, times or conditions  
605 (Fig. 8-9). Finally, climate-niche interactions also appear to explain similar early Holocene  
606 *Tsuga* declines (black circles, Fig. 6; see also Section 6.3).

607 Overall, the *Tsuga* decline appears no more dependent on disturbance agents than the  
608 regional decline of *Picea mariana* (black spruce) and other taxa during rapid climate changes at  
609 ca. 11,700 YBP after the cold Younger Dryas period, when biotic disturbance agents are rarely  
610 considered (Peteet et al., 1990; Lindbladh et al., 2007; Shuman et al., 2009). The diagnosis  
611 retains ambiguities, however. Some of our model validation statistics were low (Table 2) and  
612 some residuals large (Fig. 8-9). Other models were inaccurate (Fig. 9). Few sites have been  
613 discovered like Spruce Pond where models would predict that conditions favored abundant  
614 *Tsuga* during the classic decline period. Despite long-term conservatism of the climate niche  
615 (Fig. 5), its observed amplitude collapsed during the decline (black crosses, Fig. 6H). (The  
616 models, however, seemingly predict such an outcome by predicting the decline, Fig. 7-8).  
617 Solutions to these problems probably involve local edaphic factors, other biotic dynamics, and  
618 reconstruction uncertainties as well as the spatial mosaic of climate changes (e.g., drying in the  
619 west, but not in the east, Fig. 2B). Other climate variables like winter temperature should also be  
620 examined and may be at least as important as any other factor (Calcote, 2003).

621 Finding that climate history can predict much of *Tsuga*'s past abundance need not,  
622 however, represent a climate-versus-ecology dichotomy. The *Tsuga* decline probably represents

## Running head: Hemlock responses to Holocene climates

623 a mix of multiple proximate dynamics like those during the Younger Dryas that produced abrupt  
624 ecological changes up to 100 yrs ahead of the peak rates of climate change (Williams et al.,  
625 2002), responses to asynchronous changes in multiple climate variables (Rach et al., 2014), and  
626 asynchronous changes across sites (Gonzales and Grimm 2009). Further work should examine  
627 how interacting processes from rapid disturbance-induced mortality to long reductions in  
628 regeneration played important albeit potentially neutral roles, interchangeably facilitating the  
629 climate driven outcomes across large pollen source areas.

630

### 631 6.3 Understanding the enigmas of *Tsuga*'s Holocene history

632 Our analysis reveals that detailed knowledge of both the multivariate climate history and  
633 the complexity of the climate niche can also help to diagnose many of the enigmas of the fossil  
634 record of *Tsuga* even if some of the proximate dynamics remain unclear:

635 **The complex relationship to Holocene droughts:** *Tsuga* abundance depends upon  
636 multiple climate variables, and a change in one variable does not always coincide with a change  
637 in other (Fig. 2, 7)(Rach et al., 2014). Likewise, the interactions among climate variables can  
638 produce more severe outcomes and less intuitive changes than expected from one variable alone  
639 (see the example site trajectory as projected with respect to either moisture or temperature alone  
640 in Fig. 3A).

641 Consequently, rapid cooling across the region by  $5200 \pm 100$  YBP overlapped in time with  
642 and appears to explain most of the local *Tsuga* declines at  $5280 \pm 180$  YBP (Shuman et al., 2009),  
643 even though drought (a decline from the long-term moisture increase spanning the Holocene) did  
644 not become widespread until 4925-4575 YBP (Fig. 2C)(Booth et al., 2012; Newby et al., 2014).  
645 The cooling interacted with low effective precipitation even before the onset of the multi-century

## Running head: Hemlock responses to Holocene climates

646 drought because the long-term increase in effective precipitation had not yet reached modern  
647 levels (Fig. 2B). The interaction explains why the droughts associated with the *Tsuga* decline  
648 were only modest (100 to 150 mm anomalies) compared to the large deviation from modern  
649 effective precipitation before ca. 8000 YBP (>300 mm; Fig. 2B). Paleoclimate reconstructions  
650 from Michigan and Wisconsin indicate that similar trends extended to *Tsuga*'s western range  
651 limit (Calcote, 2003) and thus can explain range-wide changes.

652 The decline likely had multiple contributing causes (Booth et al., 2012), but they were  
653 probably multiple, independently changing climate variables (Calcote, 2003)(Fig. 7). High  
654 temperatures were required to sustain high *Tsuga* pollen percentages before the decline because  
655 effective precipitation was low and some combination of physiological, developmental,  
656 ecological, and population factors underlie a negative correlation between temperature and  
657 precipitation in the climate niche (Fig. 4C). Consequently, a sharp drop in temperatures then  
658 combined with the persistently lower-than-modern effective precipitation in the mid-Holocene to  
659 reduce the potential for high *Tsuga* abundance and cause the decline (Fig. 7). Later, increased  
660 effective precipitation enabled *Tsuga* populations to recover because temperatures remained low.  
661 Like the bold arrows in Fig. 3A, temperature could cause the decline, but moisture could later  
662 move sites back to favorable (cool, moist) portions of the climate niche.

663 **Difference in timing of the *Tsuga* decline across sites:** Spruce and Sutherland ponds  
664 represent two extremes in the local timing of the *Tsuga* decline (3975 and 5600 YBP  
665 respectively; Table 1), but differences of centuries also appear to exist between other sites such  
666 as Knob Hill and Deep ponds (5500 and 5150 YBP respectively; Fig. 2B). The interaction of  
667 three factors explains the differences: 1) spatial variability in temperature change such as rapid  
668 early cooling in the north at 5400 YBP that was briefly counteracted by warming at 5250-5200

## Running head: Hemlock responses to Holocene climates

669 YBP in the south (Fig. 2A); 2) earlier drought onset in the west than in the east (at 5800 versus  
670 5050 YBP at Davis and Deep ponds respectively; see Newby et al., 2014 for statistical analysis  
671 of this asynchrony)(Fig. 2B); and 3) differences in the relationship between *Tsuga*'s climate  
672 preferences and the absolute temperatures or effective precipitation at each site (e.g., between  
673 high versus low elevation sites such as Sutherland and Spruce ponds).

674 For example, as the Hudson Highlands cooled and dried after 5650 YBP, *Tsuga* pollen  
675 percentages declined at Sutherland Pond, which was higher and wetter than Spruce Pond where  
676 *Tsuga* pollen percentages modestly increased until further cooling at 4050 YBP (associated with  
677 cooling in the Gulf Stream region recorded by core GGC19, Fig. 2A). The decline at Sutherland  
678 Pond (5600 YBP at 380 m elevation) before Spruce Pond (at 3975 YBP at 223 m elevation)  
679 provides evidence for a downslope shift in the Hudson Highlands consistent with expectations  
680 associated with cooling. The subsequent cooling at ca. 4000 YBP not only facilitated the late  
681 *Tsuga* decline at Spruce Pond (Fig. 9H), but also an apparently synchronous *Quercus* decline at  
682 Sutherland Pond and a rapid *Betula* increase at Spruce and Sutherland ponds (Maenza-Gmelch,  
683 1997). Likewise, the earlier cooling off Nova Scotia (red line, Fig. 2A) helps to explain why both  
684 *Tsuga* and *Quercus* declined on Cape Cod at Deep Pond at 5150 YBP (Foster et al., 2006;  
685 Marsicek et al., 2013).

686 In addition to contributing to variations in the timing of the decline, short-lived climate  
687 variations could have also contributed to short-lived declines in *Tsuga* pollen percentages, such  
688 as before the classic decline at Knob Hill and other sites (Booth et al., 2012; Oswald and Foster,  
689 2012) and after brief maxima at ca. 4300 and 3000 YBP at Deep Pond (Fig. 8C). Such variability  
690 in *Tsuga* pollen percentages may be the result of intrinsic population or ecological dynamics  
691 (Williams et al., 2011), but the models show the potential for direct or indirect effects of cold or

## Running head: Hemlock responses to Holocene climates

692 drought (Fig. 7-8). Because cooling could explain some of the declines, such as after 6250 YBP  
693 (Fig. 7-9), drought indicators may not have recorded such events (Booth et al., 2012) and, as  
694 with the classic decline, comparisons of the pollen data with only drought indicators could create  
695 misleading mismatches.

696           **A unique range-wide decline rather than a shift in distribution:** At the broad scale,  
697 the rapid mid-Holocene decline fits the concept of a “crash” of the realized niche (black crosses,  
698 Fig. 6H) because *Tsuga* declined rather than experiencing a range shift (Breshears et al., 2008;  
699 Lenoir and Svenning, 2014). The negative correlation between July temperatures and annual  
700 precipitation in the climatic niche of *Tsuga* favored declines in all areas of high abundance when  
701 climate changes involved positive correlations in the two climate variables (i.e., a reduction in  
702 both temperature and precipitation by 4900 YBP; Fig. 5A, bold lines). Because the niche is  
703 anisotropic (directionally dependent and not symmetric), climate trajectories perpendicular to the  
704 niche orientation limited the number of locations where conditions remained optimal for *Tsuga*  
705 populations.

706           Had the trajectories followed the directionality of the niche (e.g., cooling coinciding with  
707 increased moisture as occurred after 2100 YBP), high abundance could have been maintained.  
708 When cooling and drying began in the mid-Holocene, however, few fossil pollen sites were  
709 warmer and wetter than those in New England, but such environments would have been required  
710 to facilitate local increases in *Tsuga* abundance. Spruce Pond, NY, which today is one of the  
711 wettest of our study sites and has the highest maximum temperatures (Table 1), may be one of  
712 the few sites to meet this criterion. However, other low-elevation sites in eastern New York may  
713 also have delayed or missing declines (Ibe, 1982); interpolation of calibrated radiocarbon ages

## Running head: Hemlock responses to Holocene climates

714 from Heart's Content Bog, New York, places the decline there at 3700 (3400-4100) YBP,  
715 although a hiatus may interrupt the bog stratigraphy (Ibe and Pardi, 1985).

716 Correlations among temperature and precipitation in the niche were probably as  
717 significant as dispersal, biotic interactions, or other factors for limiting the species' movement  
718 because the species could not move into regions with optimal temperatures if precipitation was  
719 limiting, and vice versa. The available combinations of temperature and precipitation favored  
720 only low abundance (Fig. 7), and interactions with low winter temperatures may have further  
721 limited *Tsuga*'s success (Calcote, 2003). Possibly because of antagonistic correlations among the  
722 genetic bases for certain plant traits (Etterson and Shaw, 2001), antagonistic relationships within  
723 the niche ensured that no large area existed with a suitable combination of temperature and  
724 precipitation for abundant *Tsuga* populations from ca. 5200-4000 YBP.

725 The range-wide collapse has been considered a unique and diagnostic aspect of the *Tsuga*  
726 decline (Davis, 1981), but it is similar to several other past biogeographic changes. For example,  
727 tree species, such as *Fraxinus* and *Ulmus*, which formed novel (no analog) forest assemblages  
728 during the late Pleistocene and early Holocene, also declined across their ranges. Like *Tsuga*,  
729 they declined as new combinations of multiple climate variables throughout eastern North  
730 America became inconsistent with realizing the highest amplitude portions of their niches  
731 (Williams et al., 2001; Veloz et al., 2012). *Tsuga*'s decline was more rapid than the earlier 'no  
732 analog' declines only because the pace of the relevant climate change was rapid (Fig. 7).

733 The alignment of *Tsuga*'s niche and subsequent climate trajectories also created a unique  
734 range-wide recovery. The recovery parallels the rise of other taxa, such as *Castanea*, which were  
735 the climatic opposites of the 'no analog' taxa and were initially suppressed by early Holocene  
736 conditions. They helped to form new plant communities in the late-Holocene after previously

## Running head: Hemlock responses to Holocene climates

737 having limited ranges and widespread low abundance (Webb III, 1988). Differences in the  
738 species' climate niches may explain why only *Tsuga* combined the patterns of the no-analog and  
739 novel late-Holocene taxa.

740 Consistent with this interpretation, shifts in the geographic distribution of *Tsuga* at other  
741 times during the Holocene coincided with different climate trajectories than those associated  
742 with the classic decline (bold versus thin lines in Fig. 5A). For example, after ca. 4000 YBP, a  
743 negative correlation in the change in temperature and precipitation followed the directionality of  
744 the niche (Fig. 5A). The trend toward cool and wet conditions corresponded with a renewed  
745 westward expansion of *Tsuga*'s range beyond Lake Michigan (Davis et al., 1986). *Tsuga*  
746 colonized new western sites that were dry where it was warm and wet where it was cool  
747 (Calcote, 2003), and thus, tracked a negative correlation between temperature and precipitation  
748 like that observed in the climate niche (Fig. 5). Midwestern sites had been both warmer and drier  
749 than New England due to their continental position. For this reason, they would have occupied  
750 the lower right of Fig. 5 for much of the early Holocene, and would not have been initially  
751 suitable for *Tsuga* until conditions cooled and became wetter than before, especially after ca.  
752 3000 YBP (up and left in Fig. 5A).

753 **Early-Holocene peaks and declines in only some records:** The interaction of the  
754 climate trajectories with the complexities of the niche also explains brief peaks in *Tsuga* pollen  
755 percentages before ca. 9800 YBP (Zhao et al., 2010; e.g., at Sutherland and Spruce ponds, Fig.  
756 2B). When *Tsuga* first increased in New England, the climate trajectories did not align with the  
757 anisotropy of the niche (Fig. 5A). Based on the available paleoclimate data, a rapid increase in  
758 effective precipitation corresponded with warming, and thus, cut across the alignment of *Tsuga*'s  
759 maximum abundance. Consequently, many first increases were short lived. The increases also

## Running head: Hemlock responses to Holocene climates

760 correspond to the negative mode of the distribution, dominant in the Great Lakes region today  
761 (black circles before 9000 YBP in Fig. 6). Some sites like Little and Guilder ponds (Fig. 6A,F)  
762 experienced these conditions at ca. 10,500-10,000 YBP whereas other sites like Sutherland Pond  
763 (Fig. 6C) reached the same absolute conditions and peak percentages earlier (Fig. 6). Percentages  
764 declined after ca. 10,000 YBP as the climate trajectories crossed out of the climatic region of the  
765 negative mode and into the trough in abundance between modes (see the transition from black  
766 outlined to colored symbols in Fig. 6, which marks 9000 YBP). Percentages then increased again  
767 as the trajectories moved into the climate space of the positive mode dominant in New England  
768 today (Fig. 5-6, Supplementary Animation).

769 The absence of an early peak at Knob Hill Pond (Fig. 7-9) supports this interpretation.  
770 Combinations of temperature and effective precipitation at the site persistently remained like  
771 those associated with the negative (Midwestern) group of populations today (black, Fig. 6E), and  
772 *Tsuga* abundance at Knob Hill increased only after 9800 YBP as it declined from the early peaks  
773 in southern New England (Fig. 8A, see also black symbols in the Supplementary Animation).  
774 The increase in Vermont, therefore, could represent part of the northwestward shift in  
775 populations that ultimately spread the negative group into the Midwest. As a result, the  
776 anisotropy of the niche helps to explain the mid-Holocene decline, but the bimodality in the  
777 niche explains the early peaks and declines of *Tsuga* before ca. 9800 YBP (Zhao et al., 2010).  
778

### 779 6.4 Considering multivariate climate change

780 The relationships in our data indicate that understanding vegetation biogeography at the  
781 time scale of the Holocene requires a nuanced and quantitative view of climate history. Multiple  
782 aspects of climate changed over this time period. We have not fully constrained that history here

## Running head: Hemlock responses to Holocene climates

783 (e.g., winter temperatures, seasonal precipitation rates, and the frequencies of extreme events are  
784 among the unconstrained variables), but reconstructions of two key variables (summer  
785 temperature and effective precipitation) explain much of the variation in the pollen data without  
786 evoking processes that were disconnected from climate. Consequently, multivariate climate  
787 change may be a primary ecological force at spatiotemporal scales larger than centuries and  
788 landscapes. Alternative hypotheses cannot ignore the dynamic climate history, and  
789 interpretations must consider that incomplete reconstructions of the paleoclimates (e.g., missing  
790 variables, non-linear indices, records of aquatic rather than terrestrial conditions) can emphasize  
791 misleading relationships between climate and vegetation. Our results confirm that some  
792 paleoecological dynamics, interpreted as a function of non-climatic factors (e.g., diseases,  
793 dispersal lags), may have involved climate in important ways that become evident once more  
794 than one climate variable is considered.

795

### 796 **7. Conclusions**

797 Holocene biogeography depends as much on climate as on ecology. The Holocene  
798 history of *Tsuga canadensis* reveals that interactions of multivariate climate changes with  
799 species' climate niches probably acted as a first-order control on vegetation history. Independent  
800 Holocene and modern realizations of *Tsuga*'s niche share important features and indicate that the  
801 relationships between climate and *Tsuga* abundance remained stable through time. Consequently,  
802 models of the niche based on independent reconstructions of temperature and precipitation  
803 explain 29-85% of the variance in *Tsuga* pollen percentages including the rapid, range-wide  
804 decline of *Tsuga* at ca. 5700-5000 YBP. When regional "leave-one-out" models failed to

## Running head: Hemlock responses to Holocene climates

805 reproduce this history, they did so because they did not completely or accurately represent the  
806 major features of the climate niche, such as its biomodality.

807 The *Tsuga* decline has been attributed to non-climatic factors (Davis, 1981; Booth et al.,  
808 2012), but our reconstructions indicate that it coincided with rapid regional cooling when  
809 effective precipitation was lower than today. Because *Tsuga*'s climate niche contains a negative  
810 correlation between optimal July temperatures and annual precipitation, cooling would have had  
811 to coincide with increased precipitation to sustain high abundance. Instead, drought associated  
812 with the rapid cooling prevented optimal conditions from developing at most sites until effective  
813 precipitation increased in later millennia. While undetectable biotic factors almost certainly  
814 played a role in *Tsuga*'s history, we found no direct evidence of such dynamics at the spatial and  
815 temporal scales represented by wind-dispersed pollen. Sustained bimodality in the niche further  
816 clarifies that many pollen records include an early peak in *Tsuga* abundance before ca. 9800  
817 YBP because the region briefly experienced climate conditions consistent with the Great Lakes  
818 mode of *Tsuga* abundance today. As a result, recent forest declines driven by climate changes  
819 have precedents in both early- and mid-Holocene declines of *Tsuga*, but recent declines of other  
820 taxa (e.g., *Castanea*, *Ulmus*) attributable to exotic diseases, insects, and other factors do not.

821

### 822 Acknowledgements

823 Funding for this project was provided to BS, WWO, and DRF from the National Science  
824 Foundation Ecosystem Science Program (DEB-1146297, DEB-1146207). We also benefited  
825 from thoughtful comments on the manuscript from T. Webb, J. Williams, M. Fitzpatrick, E.  
826 Currano and three anonymous reviewers. Data were obtained from the Neotoma Paleoecology

## Running head: Hemlock responses to Holocene climates

827 Database (<http://www.neotomadb.org>), and the work of the data contributors and the Neotoma  
828 community is gratefully acknowledged.

829

830

## Running head: Hemlock responses to Holocene climates

### 831 References Cited

- 832 Allen, C.D., Macalady, A.K., Chenchouni, H., Bachelet, D., McDowell, N., Vennetier, M.,  
833 Kitzberger, T., Rigling, A., Breshears, D.D., Hogg, E.H., Gonzalez, P., Fensham, R.,  
834 Zhang, Z., Castro, J., et al., 2010, A global overview of drought and heat-induced tree  
835 mortality reveals emerging climate change risks for forests: *Forest Ecology and*  
836 *Management*, v. 259, p. 660–684, doi: 10.1016/j.foreco.2009.09.001.
- 837 Allison, T.D., Moeller, R.E., and Davis, M.B., 1986, Pollen in laminated sediments provides  
838 evidence for a mid-Holocene forest pathogen outbreak: *Ecology*, v. 67, p. 1101–  
839 1105.
- 840 Anderson, R.S., Davis, R.B., Miller, N.G., and Stuckenrath, R., 1986, History of late- and post-  
841 glacial vegetation and disturbance around Upper South Branch Pond, northern  
842 Maine: *Canadian Journal of Botany*, v. 64, p. 1977–1986.
- 843 Bennett, K.D., and Fuller, J.L., 2002, Determining the age of the mid-Holocene *Tsuga cana*  
844 densis (hemlock) decline, eastern North America: *The Holocene*, v. 12, p. 421–429,  
845 doi: 10.1191/0959683602hl556rp.
- 846 Bhiry, N., and Filion, L., 1996, Mid-Holocene hemlock decline in eastern North America  
847 linked with phytophagous insect activity: *Quaternary Research*, v. 45, p. 312.
- 848 Booth, R.K., Brewer, S., Blaauw, M., Minckley, T.A., and Jackson, S.T., 2012, Decomposing the  
849 mid-Holocene *Tsuga* decline in eastern North America: *Ecology*, v. 93, p. 1841–1852,  
850 doi: 10.1890/11-2062.1.
- 851 Brassell, S.C., Eglinton, G., Marlowe, I.T., Pflaumann, U., and Sarnthein, M., 1986, Molecular  
852 stratigraphy: a new tool for climatic assessment: *Nature*, v. 320, p. 129–133.
- 853 Breshears, D.D., Cobb, N.S., Rich, P.M., Price, K.P., Allen, C.D., Balice, R.G., Romme, W.H.,  
854 Kastens, J.H., Floyd, M.L., Belnap, J., Anderson, J.J., Myers, O.B., and Meyer, C.W., 2005,  
855 Regional vegetation die-off in response to global-change-type drought: *Proceedings*  
856 *of the National Academy of Sciences of the United States of America*, v. 102, p.  
857 15144–15148.
- 858 Breshears, D.D., Huxman, T.E., Adams, H.D., Zou, C.B., and Davison, J.E., 2008, Vegetation  
859 synchronously leans upslope as climate warms: *Proceedings of the National*  
860 *Academy of Sciences*, v. 105, p. 11591–11592, doi: 10.1073/pnas.0806579105.
- 861 Broennimann, O., Treier, U.A., Müller-Schärer, H., Thuiller, W., Peterson, A.T., and Guisan, A.,  
862 2007, Evidence of climatic niche shift during biological invasion: *Ecology Letters*, v.  
863 10, p. 701–709, doi: 10.1111/j.1461-0248.2007.01060.x.
- 864 Brubaker, L.B., 1975, Postglacial forest patterns associated with till and outwash in  
865 northcentral upper Michigan: *Quaternary Research*, v. 5, p. 499–527.

Running head: Hemlock responses to Holocene climates

- 866 Calcote, R., 2003, Mid-Holocene climate and the hemlock decline: the range limit of *Tsuga*  
867 *canadensis* in the western Great Lakes region, USA: *The Holocene*, v. 13, p. 215.
- 868 Calder, W.J., and Shuman, B., 2017, Extensive wildfires, climate change, and an abrupt state  
869 change in subalpine ribbon forests, Colorado: *Ecology*, doi: 10.1002/ecy.1959.
- 870 Clark, J.S., Royall, P.D., and Chumbley, C., 1996, The Role of Fire During Climate Change in an  
871 Eastern Deciduous Forest at Devil's Bathtub, New York: *Ecology*, v. 77, p. 2148–  
872 2166.
- 873 Cleveland, W.S., 1979, Robust Locally Weighted Regression and Smoothing Scatterplots:  
874 *Journal of the American Statistical Association*, v. 74, p. 829–836, doi:  
875 10.1080/01621459.1979.10481038.
- 876 Crimmins, S.M., Dobrowski, S.Z., Greenberg, J.A., Abatzoglou, J.T., and Mynsberge, A.R., 2011,  
877 Changes in Climatic Water Balance Drive Downhill Shifts in Plant Species' Optimum  
878 Elevations: *Science*, v. 331, p. 324–327, doi: 10.1126/science.1199040.
- 879 Daly, C., Halbleib, M., Smith, J.I., Gibson, W.P., Doggett, M.K., Taylor, G.H., Curtis, J., and  
880 Pasteris, P.P., 2008, Physiographically sensitive mapping of climatological  
881 temperature and precipitation across the conterminous United States: *International  
882 Journal of Climatology*, v. 28, p. 2031–2064, doi: 10.1002/joc.1688.
- 883 Davis, M.B., 1981, Outbreaks of forest pathogens in Quaternary history: *Proceedings of the  
884 Fourth International Palynological Conference*, v. 3, p. 216–227.
- 885 Davis, M.B., and Shaw, R.G., 2001, Range Shifts and Adaptive Responses to Quaternary  
886 Climate Change: *Science*, v. 292, p. 673–679, doi: 10.1126/science.292.5517.673.
- 887 Davis, M.B., Spear, R.W., and Shane, L.C.K., 1980, Holocene climate of New England:  
888 *Quaternary Research*, v. 14, p. 240–250.
- 889 Davis, M.B., Woods, K.D., Webb, S.L., and Futyma, R.P., 1986, Despersal versus climate:  
890 Expansion of *Fagus* and *Tsuga* into the Upper Great Lakes region: *Vegetatio*, v. 67, p.  
891 93–103.
- 892 Deevey, E.S., 1943, Additional pollen analyses from southern New England: *American  
893 Journal of Science*, v. 241, p. 717–752.
- 894 Eickmeier, W., Adams, M., and Lester, D., 1975, Two physiological races of *Tsuga canadensis*  
895 in Wisconsin: *Canadian Journal of Botany*, v. 53, p. 940–951, doi: 10.1139/b75-112.
- 896 Etterson, J.R., and Shaw, R.G., 2001, Constraint to Adaptive Evolution in Response to Global  
897 Warming: *Science*, v. 294, p. 151–154, doi: 10.1126/science.1063656.
- 898 Foster, D.R., 2014, *Hemlock: A Forest Giant on the Edge*: Yale University Press, 336 p.

## Running head: Hemlock responses to Holocene climates

- 899 Foster, D.R., Oswald, W.W., Faison, E.K., Doughty, E.D., and Hansen, B.C.S., 2006, A climatic  
900 driver for abrupt mid-Holocene vegetation dynamics and the hemlock decline in  
901 New England: *Ecology*, v. 87, p. 2959–2966.
- 902 Fuller, J.L., Foster, D.R., McLachlan, J.S., and Drake, N., 1998, Impact of Human Activity on  
903 Regional Forest Composition and Dynamics in Central New England: *Ecosystems*, v.  
904 1, p. 76–95.
- 905 Gaston, K.J., 2003, The Structure and Dynamics of Geographic Ranges (Oxford Series in  
906 Ecology and Evolution) (Anonymous, Ed.): Oxford, Oxford University Press.
- 907 Gaudreau, D.C., 1986, Late-Quaternary vegetational history of the Northeast: palaeoecological  
908 implications of topographic patterns in pollen data: Yale University.,
- 909 Goerlich, D.L., and Nyland, R.D.;, 2000, Natural regeneration of eastern hemlock: a review,  
910 *in p. 14–22, https://www.treesearch.fs.fed.us/pubs/14633* (accessed February  
911 2017).
- 912 Goring, S.J., Mladenoff, D.J., Cogbill, C.V., Record, S., Paciorek, C.J., Jackson, S.T., Dietze, M.C.,  
913 Dawson, A., Matthes, J.H., McLachlan, J.S., and others, 2016, Novel and Lost Forests in  
914 the Upper Midwestern United States, from New Estimates of Settlement-Era  
915 Composition, Stem Density, and Biomass: *PloS one*, v. 11, p. e0151935.
- 916 Goring, S.J., and Williams, J.W., 2017, Effect of historical land-use and climate change on  
917 tree-climate relationships in the upper Midwestern United States: *Ecology Letters*, v.  
918 20, p. 461–470, doi: 10.1111/ele.12747.
- 919 Graham, R.W., and Grimm, E.C., 1990, Effects of Global Climate Change on the Patterns of  
920 Terrestrial Biological COMMUNITIES: *Trends in Ecology and Evolution*, v. 5, p. 289–  
921 292.
- 922 Granger, C.W.J., and Newbold, P., 1974, Spurious regressions in econometrics: *Journal of  
923 Econometrics*, v. 2, p. 111–120.
- 924 Grimm, E.C., 2010, North American Pollen Database:
- 925 Grubb, P.J., 1977, The Maintenance of Species-Richness in Plant Communities: The  
926 Importance of the Regeneration Niche: *Biological Reviews*, v. 52, p. 107–145, doi:  
927 10.1111/j.1469-185X.1977.tb01347.x.
- 928 Haas, J.N., and McAndrews, J.H., 1999, The summer drought related hemlock (*Tsuga  
929 canadensis*) decline in Eastern North America 5700 to 5100 years ago, *in* McManus,  
930 K. ed., *Symposium on Sustainable Management of Hemlock Ecosystems in Eastern  
931 North America*, United States Department of Agriculture, Forest Service,  
932 Northeastern Research Station, General Technical Report NE-267, v. Durham, New  
933 Hampshire, p. 81.

## Running head: Hemlock responses to Holocene climates

- 934 Haslett, J., and Parnell, A., 2008, A simple monotone process with application to  
935 radiocarbon-dated depth chronologies: Journal of the Royal Statistical Society:  
936 Series C (Applied Statistics), v. 57, p. 399–418, doi: 10.1111/j.1467-  
937 9876.2008.00623.x.
- 938 Hou, J., Huang, Y., Wang, Y., Shuman, B., Oswald, W., Faison, E., and Foster, D., 2006,  
939 Postglacial climate reconstruction based on compound-specific D/H ratios of fatty  
940 acids from Blood Pond, New England: Geochemistry, Geophysics, Geosystems, v. 7, p.  
941 Q03008, doi: 10.1029/2005GC001076.
- 942 Huang, Y., Shuman, B., Wang, Y., and Webb, T., 2002, Hydrogen isotope ratios of palmitic  
943 acid in lacustrine sediments record late-Quaternary climate variations: Geology, v.  
944 30, p. 1103–1106.
- 945 Ibe, R.A., 1982, Quaternary palynology of five lacustrine deposits in the Catskill Mountain  
946 region of New York: Dissertation. New York University, New York, New York, USA.
- 947 Ibe, R.A., and Pardi, R. R., 1985, A radiocarbon-dated pollen diagram for Heart's Content  
948 Bog, Green County, New York: Northeastern Geology, v. 7, p. 201-208
- 949 Jackson, S.T., and Whitehead, D.R., 1991, Holocene Vegetation Patterns in the Adirondack  
950 Mountains: Ecology, v. 72, p. 641.
- 951 Kaplan, A., Cane, M., Kushnir, Y., Clement, A., Blumenthal, M., and Rajagopalan, B., 1998,  
952 Analyses of global sea surface temperature 1856-1991: Journal of Geophysical  
953 Research, v. 103, p. 18,567-18,589.
- 954 Kessell, S.R., 1979, Adaptation and dimorphism in eastern hemlock, *Tsuga canadensis* (L.)  
955 Carr: American Naturalist, p. 333–350.
- 956 Kim, Y.-J., and Gu, C., 2004, Smoothing spline Gaussian regression: more scalable  
957 computation via efficient approximation: Journal of the Royal Statistical Society:  
958 Series B (Statistical Methodology), v. 66, p. 337–356, doi: 10.1046/j.1369-  
959 7412.2003.05316.x.
- 960 Kirby, M.E., Mullins, H.T., Patterson, W.P., and Burnett, A.W., 2002, Late glacial-Holocene  
961 atmospheric circulation and precipitation in the northeast United States inferred  
962 from modern calibrated stable oxygen and carbon isotopes: Geological Society of  
963 America Bulletin, v. 114, p. 1326–1340, doi: 10.1130/0016-  
964 7606(2002)114<1326:lghaca>2.0.co;2.
- 965 Krueger, L.M., and Peterson, C.J., 2006, Effects of White-tailed Deer on *Tsuga canadensis*  
966 Regeneration: Evidence of Microsites as Refugia from Browsing: The American  
967 Midland Naturalist, v. 156, p. 353–362, doi: 10.1674/0003-  
968 0031(2006)156[353:EOWDOT]2.0.CO;2.

## Running head: Hemlock responses to Holocene climates

- 969 Kurz, W.A., Dymond, C.C., Stinson, G., Rampley, G.J., Neilson, E.T., Carroll, A.L., Ebata, T., and  
970 Safranyik, L., 2008, Mountain pine beetle and forest carbon feedback to climate  
971 change: *Nature*, v. 452, p. 987–990.
- 972 Lenoir, J., and Svenning, J.-C., 2014, Climate-related range shifts – a global multidimensional  
973 synthesis and new research directions: *Ecography*, p. no-no, doi:  
974 [10.1111/ecog.00967](https://doi.org/10.1111/ecog.00967).
- 975 Lindbladh, M., Oswald, W.W., Foster, D.R., Faison, E.K., Hou, J., and Huang, Y., 2007, A late-  
976 glacial transition from *Picea glauca* to *Picea mariana* in southern New England:  
977 *Quaternary Research*, v. 67, p. 502–508.
- 978 Liu, Y., Brewer, S., Booth, R.K., Minckley, T.A., and Jackson, S.T., 2012, Temporal density of  
979 pollen sampling affects age determination of the mid-Holocene hemlock (*Tsuga*)  
980 decline: *Quaternary Science Reviews*, v. 45, p. 54–59, doi:  
981 [10.1016/j.quascirev.2012.05.001](https://doi.org/10.1016/j.quascirev.2012.05.001).
- 982 Maenza-Gmelch, T.E., 1997, Holocene vegetation, climate, and fire history of the Hudson  
983 Highlands, southeastern New York, USA: *The Holocene*, v. 7, p. 25–37.
- 984 Maiorano, L., Cheddadi, R., Zimmermann, N.E., Pellissier, L., Petitpierre, B., Pottier, J.,  
985 Laborde, H., Hurdu, B.I., Pearman, P.B., Psomas, A., Singarayer, J.S., Broennimann, O.,  
986 Vittoz, P., Dubuis, A., et al., 2013, Building the niche through time: using 13,000  
987 years of data to predict the effects of climate change on three tree species in Europe:  
988 *Global Ecology and Biogeography*, v. 22, p. 302–317, doi: [10.1111/j.1466-8238.2012.00767.x](https://doi.org/10.1111/j.1466-8238.2012.00767.x).
- 990 Marsicek, J.P., Shuman, B., Brewer, S., Foster, D.R., and Oswald, W.W., 2013, Moisture and  
991 temperature changes associated with the mid-Holocene *Tsuga* decline in the  
992 northeastern United States: *Quaternary Science Reviews*, v. 80, p. 129–142, doi:  
993 [10.1016/j.quascirev.2013.09.001](https://doi.org/10.1016/j.quascirev.2013.09.001).
- 994 Newby, P., Shuman, B., Donnelly, J.P., Karnauskas, K.B., and Marsicek, J.P., 2014, Centennial-  
995 to-Millennial Hydrologic Trends and Variability along the North Atlantic Coast,  
996 U.S.A., during the Holocene: *Geophys. Res. Lett.*, v. 41, doi: [10.1002/2014GL060183](https://doi.org/10.1002/2014GL060183).
- 997 Newby, P.E., Shuman, B.N., Donnelly, J.P., and MacDonald, D., 2011, Repeated century-scale  
998 droughts over the past 13,000 yrs near the Hudson River watershed, USA:  
999 *Quaternary Research*, v. 75, p. 523–530.
- 1000 Nogués-Bravo, D., 2009, Predicting the past distribution of species climatic niches: *Global*  
1001 *Ecology and Biogeography*, v. 18, p. 521–531, doi: [10.1111/j.1466-8238.2009.00476.x](https://doi.org/10.1111/j.1466-8238.2009.00476.x).
- 1003 Olson, J.S., Stearns, F.W., and Nienstaedt, H., 1959, Eastern hemlock seeds and seedlings:,  
1004 <http://agris.fao.org/agris-search/search.do?recordID=US201300607905> (accessed  
1005 February 2017).

Running head: Hemlock responses to Holocene climates

- 1006 Oswald, W.W., Doughty, E.D., Foster, D.R., Shuman, B.N., and Wagner, D.L., 2017, Evaluating  
1007 the role of insects in the middle-Holocene *Tsuga* decline: *Journal of the Torrey*  
1008 *Botanical Society*, v. 144.
- 1009 Oswald, W.W., Faison, E.K., Foster, D.R., Doughty, E.D., Hall, B.R., and Hansen, B.C.S., 2007,  
1010 Post-glacial changes in spatial patterns of vegetation across southern New England:  
1011 *Journal of Biogeography*, v. 34, p. 900–913.
- 1012 Oswald, W.W., and Foster, D.R., 2012, Middle-Holocene dynamics of *Tsuga canadensis*  
1013 (eastern hemlock) in northern New England, USA: *The Holocene*, v. 22, p. 71–78, doi:  
1014 10.1177/0959683611409774.
- 1015 Oswald, W.W., Foster, D.R., Shuman, B.N., Doughty, E.D., Faison, E.K., Hall, B.R., Hansen, B.C.,  
1016 Lindbladh, M., Marroquin, A. and Truebe, S.A., 2018, Subregional variability in the  
1017 response of New England vegetation to postglacial climate change, *Journal of*  
1018 *Biogeography*, v. 45, p. 2375-2388.
- 1019 Paciorek, C.J., Goring, S.J., Thurman, A.L., Cogbill, C.V., Williams, J.W., Mladenoff, D.J., Peters,  
1020 J.A., Zhu, J., and McLachlan, J.S., 2016, Statistically-estimated tree composition for the  
1021 northeastern United States at Euro-American settlement: *PloS one*, v. 11, p.  
1022 e0150087.
- 1023 Parnell, A.C., Haslett, J., Allen, J.R.M., Buck, C.E., and Huntley, B., 2008, A flexible approach to  
1024 assessing synchronicity of past events using Bayesian reconstructions of  
1025 sedimentation history: *Quaternary Science Reviews*, v. 27, p. 1872–1885, doi:  
1026 10.1016/j.quascirev.2008.07.009.
- 1027 Parshall, T., 2002, Late Holocene stand-scale invasion by hemlock (*Tsuga canadensis*) at its  
1028 western range limit: *Ecology*, v. 83, p. 1386.
- 1029 Peteet, D.M., Vogel, J.S., Nelson, D.E., Southron, J.R., Nickmann, R.J., and Heusser, L.E., 1990,  
1030 Younger Dryas climatic reversal in northeastern USA? AMS ages for an older  
1031 problem: *Quaternary Research*, v. 33, p. 219.
- 1032 Peterson, A.T., Soberon, J., Pearson, R.G., Anderson, R.P., Martinez-Meyer, E., Nakamura, M.,  
1033 and Araújo, M.B., 2011, *Ecological Niches and Geographic Distributions*: Princeton,  
1034 N.J, Princeton University Press, 328 p.
- 1035 Potter, K.M., Jetton, R.M., Dvorak, W.S., Hipkins, V.D., Rhea, R., and Whittier, W.A., 2012,  
1036 Widespread inbreeding and unexpected geographic patterns of genetic variation in  
1037 eastern hemlock (*Tsuga canadensis*), an imperiled North American conifer:  
1038 *Conservation Genetics*, v. 13, p. 475–498, doi: 10.1007/s10592-011-0301-2.
- 1039 Prahl, F.G., Mix, A.C., and Sparrow, M.A., 2006, Alkenone paleothermometry: Biological  
1040 lessons from marine sediment records off western South America: *Geochimica et*  
1041 *Cosmochimica Acta*, v. 70, p. 101–117, doi: 10.1016/j.gca.2005.08.023.

## Running head: Hemlock responses to Holocene climates

- 1042 Prentice, I.C., Bartlein, P.J., and Webb III, T., 1991, Vegetation and climate changes in  
1043 eastern North America since the last glacial maximum: A response to continuous  
1044 climatic forcing: *Ecology*, v. 72, p. 2038–2056.
- 1045 Prentice, I.C., Cramer, W., Harrison, S.P., Leemans, R., Monserud, R.A., and Solomon, A.M.,  
1046 1992, A global biome model based on plant physiology and dominance, soil  
1047 properties and climate: *Journal of Biogeography*, v. 19, p. 117.
- 1048 Pribyl, P., and Shuman, B.N., 2014, A computational approach to Quaternary lake-level  
1049 reconstruction applied in the central Rocky Mountains, Wyoming, USA: *Quaternary*  
1050 *Research*, v. 82, p. 249–259, doi: 10.1016/j.yqres.2014.01.012.
- 1051 R Core Team, 2017, R: A language and environment for statistical computing. R Foundation  
1052 for Statistical Computing, Vienna, Austria, <http://www.R-project.org>.
- 1053 Rach, O., Brauer, A., Wilkes, H., and Sachse, D., 2014, Delayed hydrological response to  
1054 Greenland cooling at the onset of the Younger Dryas in western Europe: *Nature*  
1055 *Geoscience*, v. 7, p. 109–112, doi: 10.1038/ngeo2053.
- 1056 Rooney, T.P., McCormick, R.J., Solheim, S.L., and Waller, D.M., 2000, Regional Variation in  
1057 Recruitment of Hemlock Seedlings and Saplings in the Upper Great Lakes, Usa:  
1058 *Ecological Applications*, v. 10, p. 1119–1132, doi: 10.1890/1051-  
1059 0761(2000)010[1119:RVIROH]2.0.CO;2.
- 1060 Sachs, J.P., 2007, Cooling of Northwest Atlantic slope waters during the Holocene: *Geophys.*  
1061 *Res. Lett.*, v. 34, p. L03609, doi: 10.1029/2006gl028495.
- 1062 Shane, L.C.K., 1991, Vegetation history of western Ohio: Limnological Research Center,  
1063 University of Minnesota, Minneapolis, Minnesota.
- 1064 Shuman, B., Bartlein, P., Logar, N., Newby, P., and Webb, T., 2002, Parallel climate and  
1065 vegetation responses to the early-Holocene collapse of the Laurentide Ice Sheet:  
1066 *Quaternary Science Reviews*, v. 21, p. 1793–1805.
- 1067 Shuman, B.N., and Burrell, S. A., 2017, Centennial to millennial hydroclimatic fluctuations in  
1068 the humid northeast United States during the Holocene: *Quaternary Research*, v. 88,  
1069 p. 514-524.
- 1070 Shuman, B.N., and Marsicek, J.P., 2016, The Structure of Holocene Climate Change in Mid-  
1071 Latitude North America: *Quaternary Science Reviews*, v. 141, p. 38–51.
- 1072 Shuman, B.N., Marsicek, J.P., Oswald, W. W., and Foster, D. R., 2019, Predictable hydrological  
1073 and ecological responses to Holocene North Atlantic variability: *Proceedings of the*  
1074 *National Academy of Sciences*, in press.

Running head: Hemlock responses to Holocene climates

- 1075 Shuman, B.N., Newby, P., and Donnelly, J.P., 2009, Abrupt climate change as an important  
1076 agent of ecological change in the Northeast U.S. throughout the past 15,000 years:  
1077 Quaternary Science Reviews, v. 28, p. 1693–1709.  
1078
- 1079 Shuman, B.N., Newby, P., Huang, Y., and Webb, T., 2004, Evidence for the close climatic  
1080 control of New England vegetation history: Ecology, v. 85, p. 1297–1310.
- 1081 Spear, R.W., 1989, Late-Quaternary History of High-Elevation Vegetation in the White  
1082 Mountains of New Hampshire: Ecological Monographs, v. 59, p. 125–151.
- 1083 Spear, R.W., Davis, M.B., and Shane, L.C.K., 1994, Lake Quaternary history of low-and mid-  
1084 elevation vegetation in the White Mountains of New Hampshire: Ecological  
1085 Monographs, v. 64, p. 85.
- 1086 Stearns, F., and Olson, J., 1958, Interactions of Photoperiod and Temperature Affecting Seed  
1087 Germination in *Tsuga canadensis*: American Journal of Botany, v. 45, p. 53–58, doi:  
1088 10.2307/2438321.
- 1089 Svenning, J.-C., and Sandel, B., 2013, Disequilibrium vegetation dynamics under future  
1090 climate change: American Journal of Botany, doi: 10.3732/ajb.1200469.
- 1091 Telford, R.J., and Birks, H.J.B., 2011, A novel method for assessing the statistical significance  
1092 of quantitative reconstructions inferred from biotic assemblages: Quaternary  
1093 Science Reviews, v. 30, p. 1272–1278, doi: 10.1016/j.quascirev.2011.03.002.
- 1094 Veloz, S.D., Williams, J.W., Blois, J.L., He, F., Otto-Bliesner, B., and Liu, Z., 2012, No-analog  
1095 climates and shifting realized niches during the late quaternary: implications for  
1096 21st-century predictions by species distribution models: Global Change Biology, v.  
1097 18, p. 1698–1713, doi: 10.1111/j.1365-2486.2011.02635.x.
- 1098 Vose, R.S., Applequist, S., Squires, M., Durre, I., Menne, M.J., Williams, C.N., Fenimore, C.,  
1099 Gleason, K., and Arndt, D., 2014, Improved Historical Temperature and Precipitation  
1100 Time Series for U.S. Climate Divisions: J. Appl. Meteor. Climatol., v. 53, p. 1232–1251,  
1101 <https://doi.org/10.1175/JAMC-D-13-0248.1>
- 1102 Wang, Y., Gill, J.L., Marsicek, J., Dierking, A., Shuman, B., and Williams, J.W., 2015,  
1103 Pronounced variations in *Fagus grandifolia* abundances in the Great Lakes region  
1104 during the Holocene: The Holocene, p. 959683615612586, doi:  
1105 10.1177/0959683615612586.
- 1106 Wang, C., Perlin, M.H., Van Stockum, J., R.R., Hamilton, C.H., and Wagner, D.B., 1997,  
1107 Chloroplast DNA polymorphisms in *Tsuga canadensis* and *Tsuga caroliniana*:  
1108 Canadian Journal of Forest Research, v. 27, p. 1329–1335, doi: 10.1139/x97-095.
- 1109 Webb, T., 1982, Temporal resolution in Holocene pollen data: Third North American  
1110 Paleontological Convention, Proceedings, v. 2, p. 569–572.

## Running head: Hemlock responses to Holocene climates

- 1111 Webb III, T., 1988, Glacial and Holocene vegetation history: Eastern North America, *in*  
1112 Huntley, B. and Webb III, T. eds., Vegetation History, Dordrecht, Kluwer Academic, p.  
1113 385–414.
- 1114 Webb III, T., 1986, Is vegetation in equilibrium with climate? How to interpret late-  
1115 Quaternary pollen data: *Vegetatio*, v. 67, p. 75–91.
- 1116 Webb III, T., Bartlein, P.J., Harrison, S.P., and Anderson, K.H., 1993, Vegetation, lake levels,  
1117 and climate in eastern North America for the past 18,000 years, *in* Wright Jr., H.E.,  
1118 Kutzbach, J.E., Webb III, T., Ruddiman, W.F., Street-Perrott, F.A., and Bartlein, P.J.  
1119 eds., Global Climates Since the Last Glacial Maximum, Minneapolis, University of  
1120 Minnesota Press, p. 415–467.
- 1121 Whitmore, J., Gajewski, K., Sawada, M., Williams, J., Shuman, B., Bartlein, P.J., Shafer, S.,  
1122 Minckley, T., Viau, A., and Brubaker, L., 2005, An updated modern pollen-climate-  
1123 vegetation dataset for North America: *Quaternary Science Reviews*, v. 24, p. 1828–  
1124 1848.
- 1125 Williams, J.W., Blois, J.L., and Shuman, B.N., 2011, Extrinsic and intrinsic forcing of abrupt  
1126 ecological change: case studies from the late Quaternary: *Journal of Ecology*, v. 99, p.  
1127 664–677, doi: 10.1111/j.1365-2745.2011.01810.x.
- 1128 Williams, J.W., Grimm, E.C., Blois, J.L., Charles, D.F., Davis, E.B., Goring, S.J., Graham, R.W.,  
1129 Smith, A.J., Anderson, M., Arroyo-Cabrales, J., and Ashworth, A.C., 2018, The Neotoma  
1130 Paleoecology Database, a multiproxy, international, community-curated data  
1131 resource: *Quaternary Research*, v. 89, p. 156–77.
- 1132 Williams, J.W., Post, D.M., Cwynar, L.C., Lotter, A.F., and Levesque, A.J., 2002, Rapid and  
1133 widespread vegetation responses to past climate change in the North Atlantic  
1134 region: *Geology*, v. 30, p. 971.
- 1135 Williams, J.W., Shuman, B., Bartlein, P.J., Whitmore, J., Gajewski, K., Sawada, M., Minckley, T.,  
1136 Shafer, S., Viau, A.E., Webb, T., Anderson, P.M., Brubaker, L.B., Whitlock, C., and Davis,  
1137 O.K., 2006, An Atlas of Pollen-Vegetation-Climate Relationships for the United States  
1138 and Canada.: American Association of Stratigraphic Palynologists Foundation,  
1139 Dallas, TX.,
- 1140 Williams, J.W., Shuman, B., and Webb, T., 2001, Dissimilarity Analyses of Late-Quaternary  
1141 Vegetation and Climate in Eastern North America: *Ecology*, v. 82, p. 3346.
- 1142 Williams, J.W., Shuman, B., Webb, T., Bartlein, P.J., and Leduc, P.L., 2004, Late Quaternary  
1143 vegetation dynamics in North America: scaling from taxa to biomes: *Ecological*  
1144 *Monographs*, v. 74, p. 309–334.
- 1145 Witt, J.C., and Webster, C.R., 2010, Regeneration dynamics in remnant *Tsuga canadensis*  
1146 stands in the northern Lake States: Potential direct and indirect effects of herbivory:

## Running head: Hemlock responses to Holocene climates

- 1147 Forest Ecology and Management, v. 260, p. 519–525, doi:  
1148 10.1016/j.foreco.2010.05.007.
- 1149 Wood, S.N., 2011, Fast stable restricted maximum likelihood and marginal likelihood  
1150 estimation of semiparametric generalized linear models: Journal of the Royal  
1151 Statistical Society: Series B (Statistical Methodology), v. 73, p. 3–36, doi:  
1152 10.1111/j.1467-9868.2010.00749.x.
- 1153 Wood, S.N., 2006a, Generalized Additive Models: An Introduction with R: Chapman and  
1154 Hall/CRC, Chapman & Hall/CRC Texts in Statistical Science, 410 p.,  
1155 <http://www.crcpress.com/product/isbn/9781584884743> (accessed January 2015).
- 1156 Wood, S.N., 2006b, Low-Rank Scale-Invariant Tensor Product Smooths for Generalized  
1157 Additive Mixed Models: Biometrics, v. 62, p. 1025–1036, doi: 10.1111/j.1541-  
1158 0420.2006.00574.x.
- 1159 Woodward, F.I., 1987, Climate and Plant Distribution (R. S. K. Barnes, H. J. B. Birks, E. F.  
1160 Connor, J. L. Harper, & R. T. Paine, Eds.): Cambridge, Cambridge University Press,  
1161 Cambridge Studies in Ecology, 174 p.
- 1162 Yu, Z., Andrews, J.H., and Eicher, U., 1997, Middle Holocene dry climate caused by change in  
1163 atmospheric circulation patterns: Evidence from lake levels and stable isotopes:  
1164 Geology, v. 25, p. 251–254.
- 1165 Zhao, Y., Yu, Z.C., and Zhao, C., 2010, Hemlock (*Tsuga canadensis*) declines at 9800 and  
1166 5300 cal yr BP caused by Holocene climatic shifts in northeastern North America:  
1167 The Holocene, v. 20, p. 877–886, doi: 10.1177/0959683610365932.
- 1168

Running head: Hemlock responses to Holocene climates

**Table 1: Study sites sorted by mean July**

**temperature**

Site	PRISM 1940-1970 normals										
	Latitude	Longitude	Elev	July Temperature (degrees C)			Precip	Dates	Samples	TSD	Reference
	Degrees	Degrees	m	Mean	Maximum	Minimum	mm	#	11 ka	YBP	
Guilder Pond	42.11	73.44	624	19.9	25.5	14.2	1111	9	41	5325	Oswald et al., (2018)
											Oswald & Foster
Knob Hill Pond	44.36	72.37	370	19.3	26.3	12.3	931	9	130	5500	(2012)
Little Pond	42.68	72.19	302	20.4	27.5	13.3	1046	7	80	5300	Oswald et al. (2007)
Mohawk Pond	41.82	73.28	360	20.8	26.5	15.1	1171	12	34	5550	Gaudreau (1986)
Blood Pond	42.08	71.96	214	21.0	26.9	15.2	1101	15	120	5200	Oswald et al. (2007)
Deep Pond	41.56	70.64	23	21.1	24.9	17.2	1125	14	140	5150	Foster et al. (2006)
Spruce Pond	41.24	74.20	223	21.9	28.1	15.7	1162	9	141	3975	Maenza-Gmelch (1997)
Sutherland Pond	41.39	74.04	380	22.1	27.4	16.7	1251	11	140	5600	Maenza-Gmelch (1997)

“Elev” refers to elevation; “Precip” refers to mean annual precipitation; “Dates” refers to the number of calibrated radiocarbon ages used to constrain the pollen sample ages; “Samples since 11ka” refers to the number of pollen samples in the record since 11,000 YBP (calendar years before CE 1950).

“TSD” refers to *Tsuga* decline age based on the peak rate of change over 100-yr intervals rounded to the nearest 25 years; ages are presented as YBP.

**Table 2. Model statistics.**

“Maximum” refers to the maximum percentage of *Tsuga* pollen at each site. “RMSE” is the root mean squared error of each model, and for the regional models refers to the error at the site excluded from the model. The regional model  $r^2_{\text{region}}$  represents the variance explained across all other sites, and  $r_{\text{site}}$  indicates the Pearson correlation coefficient of the observed versus predicted percentages at the excluded site; \* indicates  $p < 0.05$  and \*\*,  $p < 0.0005$ . The “RMSE/Max” is the proportion of the RMSE to the maximum *Tsuga* pollen percentage at each site. “Converged” represented the percentage of random models that converged without failing.

Site	Random null models			Site-specific model			Regional model with site excluded		
	Maximum (%)	$r^2$ (5-95% range)	converged (%)	$r^2$	RMSE (%)	RMSE/Max	$r^2_{\text{region}}$	$r_{\text{site}}$	RMSE (%)
Knob Hill	43	0.11-0.57	89	0.85	5.0	0.12	0.71	-0.08	16
Guilder	32	0.09-0.50	90	0.69	4.5	0.14	0.70	0.14*	10
Little	35	0.09-0.60	92	0.76	5.2	0.15	0.73	0.23**	11
<i>Deficient models</i>									
Blood	16	0.06-0.37	90	0.54	2.4	0.15	0.75	0.31**	4.3
Mohawk	22	0.06-0.48	85	0.70	3.2	0.15	0.75	0.65**	5.6
Deep	6	0.05-0.35	90	0.43	0.9	0.14	0.70	0.60**	2.1
Sutherland	16	0.03-0.25	91	0.29	1.9	0.12	0.73	0.23**	3.1
Spruce	12	0.08-0.46	90	0.54	1.8	0.15	0.73	0.13*	5
<i>Complete models</i>									

## Running head: Hemlock responses to Holocene climates

### Figure captions

Figure 1. A) Map of the percentages of *Tsuga* pollen in modern sediment samples (gray and green circles) from Whitmore et al. (2005) and the locations of records used in this study (squares, pollen; blue triangles, lake levels; red triangles, sea-surface temperatures). Gray circles represent samples from cooler and drier sites than the mean of all samples with >1% *Tsuga* pollen; green circles indicate warmer and wetter sites than the mean. B) Filled circles indicate where plant populations would have to grow today to experience climates equivalent to those reconstructed for the past at Blood Pond, Massachusetts (square), labeled by millennium before present (kYBP). The west-to-east trajectory of analogous climates passes into and out of regions with abundant *Tsuga* pollen based on the mean latitude and longitude of all modern pollen samples with July temperatures and annual precipitation within 0.5°C and 50 mm respectively of past conditions inferred from alkenone paleothermometry (Fig. 2A; Sachs, 2007) and lake-level data (Fig. 2B; Newby et al., 2014). Symbol colors represent the time period represented. Gray circles represent the modern percentages of *Tsuga* pollen as in A.

Figure 2. A) Holocene temperature changes reconstructed from alkenones from ocean cores GGC30 off Nova Scotia (red line) and GGC19 off Virginia (gray line)(Sachs, 2007). B) Effective precipitation reconstructions calculated from lake-level changes at Davis (dark blue) and Deep ponds (gray)(Marsicek et al., 2013; Newby et al., 2014). C) Representative *Tsuga* pollen time series (normalized to z-scores for visualization) with arrows highlighting enigmatic features of the record, including differences in decline timing.

## Running head: Hemlock responses to Holocene climates

Figure 3. A conceptual model shows how asymmetric, multivariate climate niches can produce non-linear and unexpected responses to linear climate trends. In A, green shading represents increased *Tsuga* abundance with respect to temperature (top in A), moisture (right in A), and the interaction of the two climate variables (lower left in A). Bold arrows in A illustrate that changes in either climate variable could result in changes in *Tsuga* abundance. The thin arrow in A represents a possible trajectory through the niche based on the climate history represented for two periods in B; the dashed lines in A show where the first period would plot and the solid line shows the second period. Because of the interaction of temperature and moisture, optimal moisture conditions may coincide with minimal *Tsuga* abundance at the boundary between periods 1 and 2, and the trajectory does not project intuitively into uni-modal climate space for either temperature or moisture.

Figure 4. Modern *Tsuga* pollen percentages plotted relative to mean July temperature and annual precipitation. Panels A and D represent the single variable projections (sides) of the bivariate climate space shown in panel C; panel B represents a projection onto the cross-cutting diagonal line in C. Panels A and D show the percentages relative to mean July temperature (T) and mean annual precipitation (P) respectively. The x-axis in B is measured as summed standard deviations from the mean values of T and P for all samples with >1% *Tsuga* pollen. As in Figure 1, gray circles represent sites that are both cooler and drier than the mean (left side of B); green circles indicate warmer and wetter sites than the mean (right side of B). Bold orange lines show the locally-weighted means

## Running head: Hemlock responses to Holocene climates

of *Tsuga* pollen percentages from all samples; dashed orange lines show the local means for cool dry samples (gray symbols) and thin solid orange lines show the local means for warm wet samples (green symbols). In C, bubble sizes represent *Tsuga* pollen percentages with largest equal to 50%.

Figure 5. Plots show *Tsuga* pollen percentages today (A), during the Holocene (B), and their differences (C, D) with respect to mean July temperature and annual precipitation and the trajectories of three study sites (colored lines in A). Green circles indicate the upper 95% of the distribution of pollen percentages within 0.5°C and 50 mm windows with the largest symbols representing 50% *Tsuga* pollen. Modern pollen percentages also appear as black circles for comparison with green Holocene values in B. Panel A includes the climate trajectories of Knob Hill (black), Blood (brown), and Spruce ponds (red) with the period of rapid regional cooling at 5600-5300 YBP in bold. The lower end of each thin line represents the oldest samples; the right end of each bold line indicates 5600 YBP and the left end indicates 5300 YBP. Panel C shows the median differences between 1000 random pairs of modern and Holocene samples within each climate window: green plus symbols, scaled to the difference like the circles in A and B, indicate a greater median value during the Holocene than today. The few black symbols indicate the reverse. Circled symbols indicate significant differences. “X” denotes windows with non-zero Holocene medians but a zero median today; gray squares indicate modern climates not experienced by the study sites during the Holocene. The histogram in D shows the differences between all randomly paired samples with vertical black lines depicting the 95% range of differences.

## Running head: Hemlock responses to Holocene climates

Figure 6. Fossil *Tsuga* pollen percentages from each study site (colored symbols) are plotted with respect to all modern samples (gray) and their climates, represented as standard deviations from the mean climate of all sites where *Tsuga* pollen percentages exceed 1% today (as in Figure 4B). Black circles represent samples older than 9000 YBP; black filled symbols represent >10,500 YBP and black outlined symbols, 10,500-9000 YBP. Black crosses indicate the 500-yr period after the decline from 5200-4700 YBP when percentages were low but retained bimodality (panel H). Because the regional climate became wetter through time (Fig. 2B), the oldest samples plot furthest left (negative departures from the mean) and the youngest samples to the right (positive departures from the mean). Sites shown are Guilder (light blue), Mohawk (dark blue), Sutherland (dark orange), Spruce (red), Knob Hill (dark gray), Little (LPR, dark green), Blood (brown), and Deep ponds (light orange). All sites are shown together in panel H. A supplementary animation shows the realized expression of these relationships by 500-yr time slice.

Figure 7. *Tsuga* pollen percentages from A) Deep and B) Knob Hill ponds (green) are shown with a climate index (orange) defined by the sum of the positive departures from the Holocene mean (z-scores) of July temperatures and annual precipitation for each site and scaled to the variance of the pollen data. The positive z-scores represent increases in either temperature or precipitation, like those represented by bold arrows in Fig. 3A, which would favor abundant *Tsuga*. The z-scores of the interpolated temperature (red) and precipitation (blue) series for each site are plotted versus time below.

## Running head: Hemlock responses to Holocene climates

Figure 8. Comparison of observed *Tsuga* pollen percentages with site-specific and regional “leave-one-out” models for Blood, Mohawk, Deep, and Sutherland ponds. Left panels show the observed pollen percentages (in green) plotted versus time with the predicted values from both the site-specific (black) and “leave-one-out” (orange) GAMs. Scatter plots compare the observed and predicted values for each site-specific model. The right-most panels represent the response surface produced by fitting a GAMM to all data from >500 YBP in the region except for the target site. Contours represent increments of 0.1 standard error (S.E.) from the mean; light shades of green represent areas of low pollen percentages and dark shades represent areas of high percentages. Black lines show the climate trajectory of each individual site relative to mean July temperatures (JulT) and annual precipitation (AnnP) with blue line segments representing the period from 5600-5300 YBP associated with the classic *Tsuga* decline. Thin black lines represent the period after 5300 YBP whereas thick black lines represent the period before 5600 YBP.

Figure 9. Same as Figure 8 but for study sites with deficient or erroneous regional “leave-one-out” models (Knob Hill, Guilder, Little, and Spruce ponds). Comparison of the surfaces in the right panels with those in Figure 8 or for Spruce Pond in D reveals truncated coverage, gaps, or misrepresentation of the bimodality in the models in A-C that target Knob Hill, Guilder, or Little ponds.

Figure 10. Histograms show the frequency of adjusted (Adj.)  $R^2$  values for GAMs generated for each site based on 100 pairs of random variables with the same temporal

## Running head: Hemlock responses to Holocene climates

autocorrelation as the reconstructed temperature and effective precipitation time series used in the site-specific GAMs (black lines in Figures 8-9). The adjusted  $R^2$  for each sites-specific (T+P) model, based on the actual climate reconstructions, is represented by a vertical dashed line.

Supplementary Animation: Plots of *Tsuga* pollen percentages along the axis of temperature-precipitation interaction as in Figure 6 shown by 500-yr time slice. Gray symbols in all panels represent modern values, but colored symbols indicate fossil samples from each site during each 500 yr period. Sites shown are Guilder (light blue), Knob Hill (black), Little (dark green), Mohawk (dark blue), Blood (brown), Deep (light green with black outline), Sutherland (orange), and Spruce ponds (red).

Running head: Hemlock responses to Holocene climates

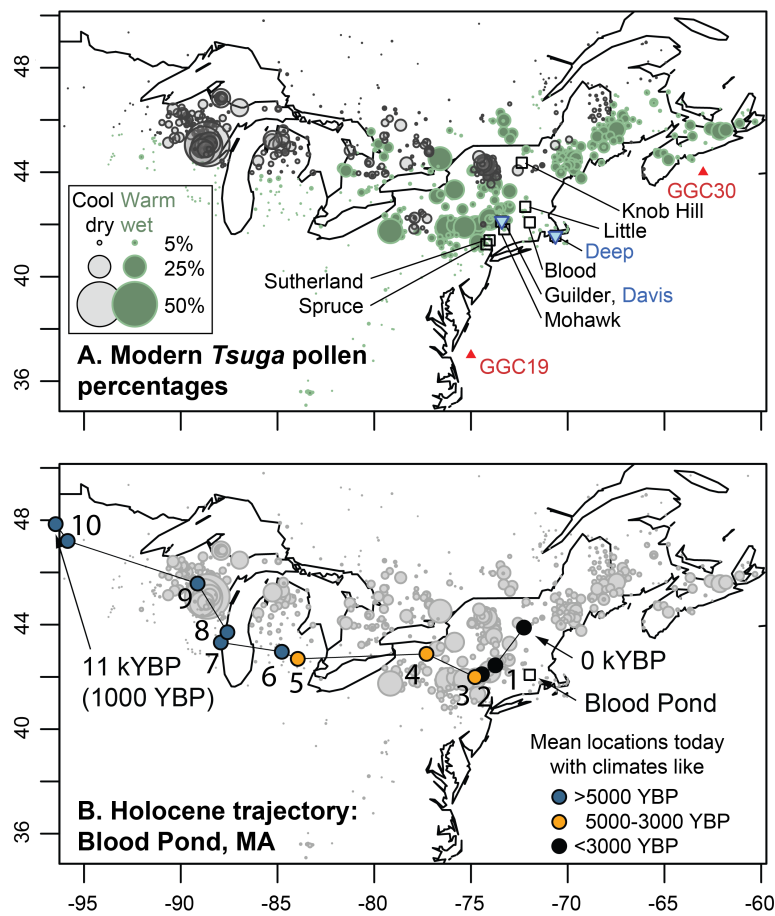


**Figure 1.** A) Map of the percentages of *Tsuga* pollen in modern sediment samples (gray and green circles) from Whitmore et al. (2005) and the locations of records used in this study (squares, pollen; blue triangles, lake levels; red triangles, sea-surface temperatures). Gray circles represent samples from cooler and drier sites than the mean of all samples with >1% *Tsuga* pollen; green circles indicate warmer and wetter sites than the mean. B) Filled circles indicate where plant populations would have to grow today to experience climates equivalent to those reconstructed for the past at Blood Pond, Massachusetts (square), labeled by millennium before present (kYBP). The west-to-east trajectory of analogous climates passes into and out of regions with abundant *Tsuga* pollen based on the mean latitude and longitude of all modern pollen samples with July temperatures and annual precipitation within 0.5°C and 50 mm respectively of past conditions inferred from alkenone paleothermometry (Fig. 2A; Sachs, 2007) and lake-level data (Fig. 2B; Newby et al., 2014). Symbol colors represent the time period represented. Gray circles represent the modern percentages of *Tsuga* pollen as in A.

## Running head: Hemlock responses to Holocene climates

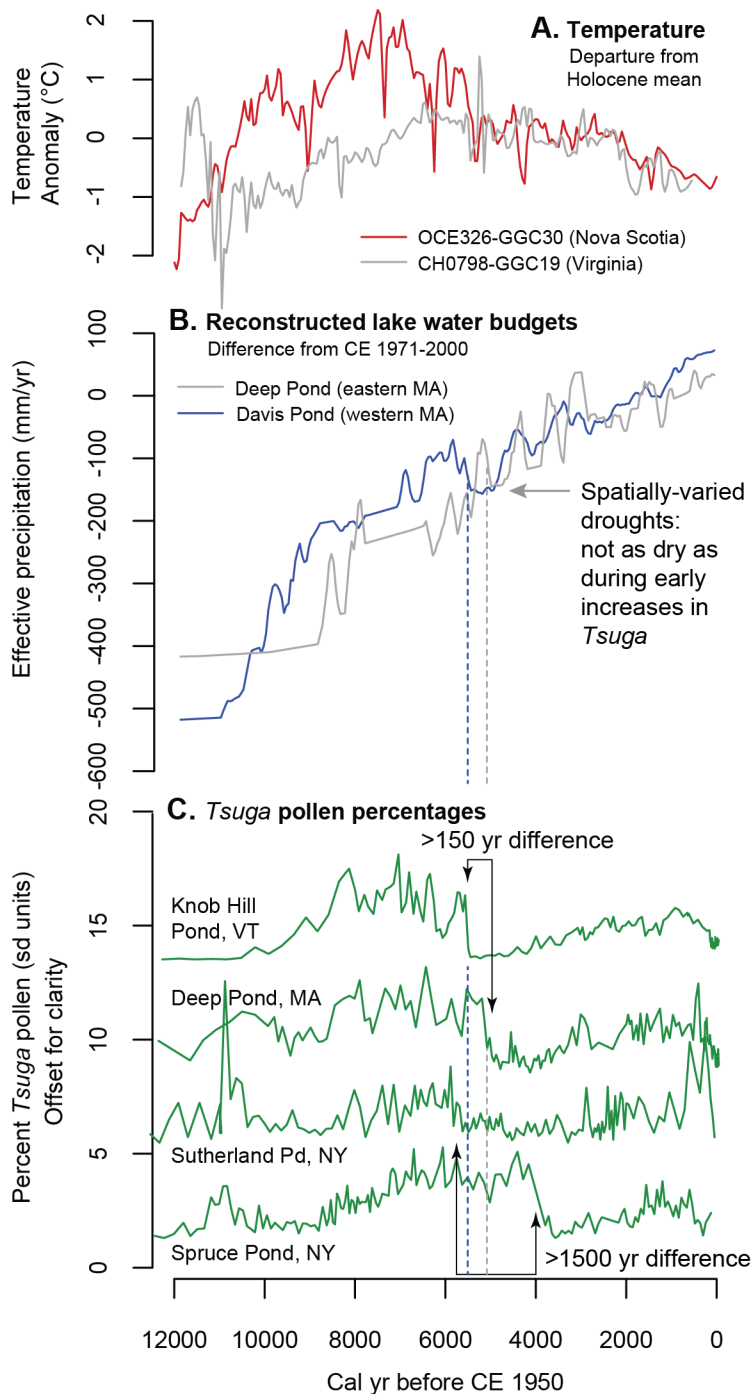


**Figure 2.** A) Holocene temperature changes reconstructed from alkenones from ocean cores GGC30 off Nova Scotia (red line) and GGC19 off Virginia (gray line)(Sachs, 2007). B) Effective precipitation reconstructions calculated from lake-level changes at Davis (dark blue) and Deep ponds (gray)(Marsicek et al., 2013; Newby et al., 2014). C) Representative *Tsuga* pollen time series (normalized to z-scores for visualization) with arrows highlighting enigmatic features of the record, including differences in decline timing.

## Running head: Hemlock responses to Holocene climates

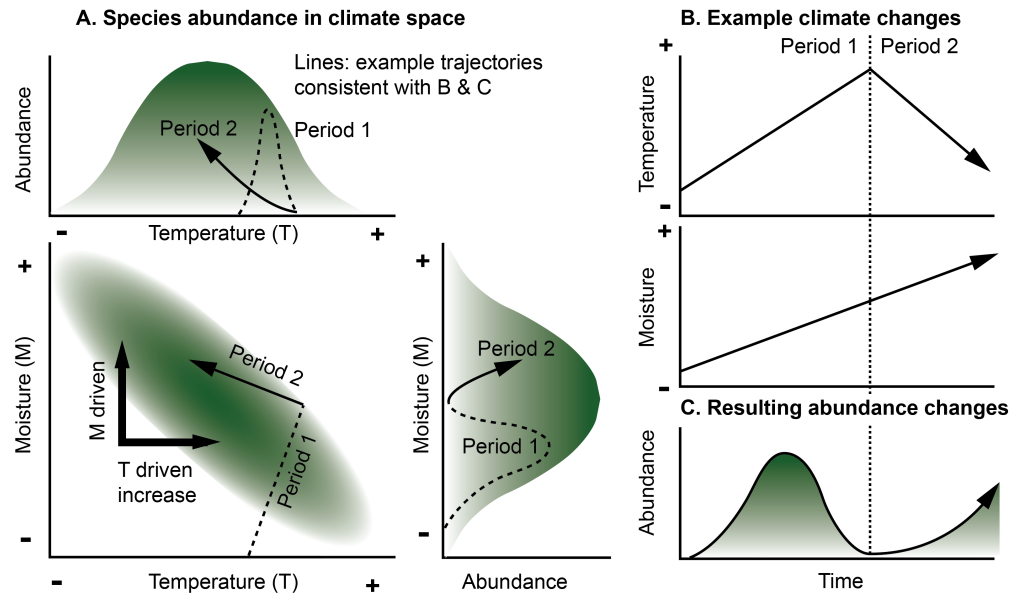


**Figure 3.** A conceptual model shows how asymmetric, multivariate climate niches can produce non-linear and unexpected responses to linear climate trends. In A, green shading represents increased *Tsuga* abundance with respect to temperature (top in A), moisture (right in A), and the interaction of the two climate variables (lower left in A). Bold arrows in A illustrate that changes in either climate variable could result in changes in *Tsuga* abundance. The thin arrow in A represents a possible trajectory through the niche based on the climate history represented for two periods in B; the dashed lines in A show where the first period would plot and the solid line shows the second period. Because of the interaction of temperature and moisture, optimal moisture conditions may coincide with minimal *Tsuga* abundance at the boundary between periods 1 and 2, and the trajectory does not project intuitively into uni-modal climate space for either temperature or moisture.

Running head: Hemlock responses to Holocene climates

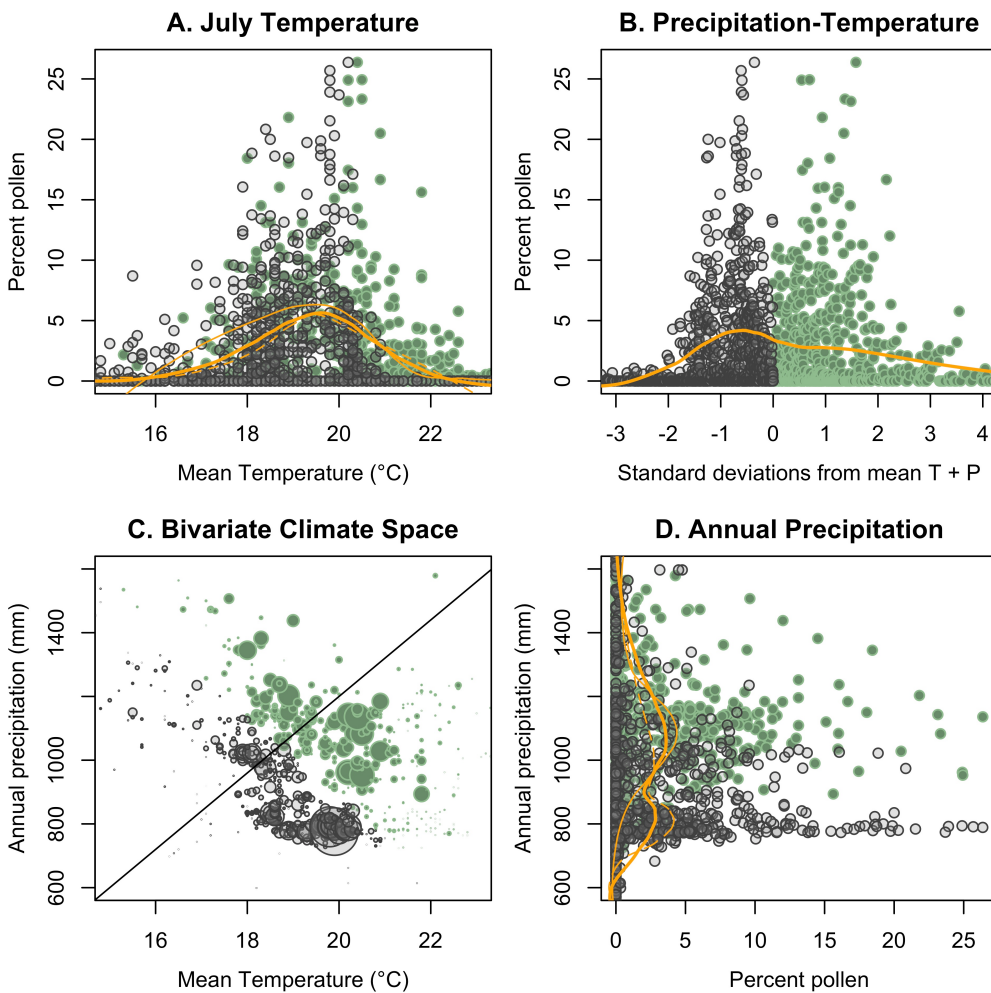


**Figure 4.** Modern *Tsuga* pollen percentages plotted relative to mean July temperature and annual precipitation. Panels A and D represent the single variable projections (sides) of the bivariate climate space shown in panel C; panel B represents a projection onto the cross-cutting diagonal line in C. Panels A and D show the percentages relative to mean July temperature (T) and mean annual precipitation (P) respectively. The x-axis in B is measured as summed standard deviations from the mean values of T and P for all samples with >1% *Tsuga* pollen. As in Figure 1, gray circles represent sites that are both cooler and drier than the mean (left side of B); green circles indicate warmer and wetter sites than the mean (right side of B). Bold orange lines show the locally-weighted means of *Tsuga* pollen percentages from all samples; dashed orange lines show the local means for cool dry samples (gray symbols) and thin solid orange lines show the local means for warm wet samples (green symbols). In C, bubble sizes represent *Tsuga* pollen percentages with largest equal to 50%.

## Running head: Hemlock responses to Holocene climates

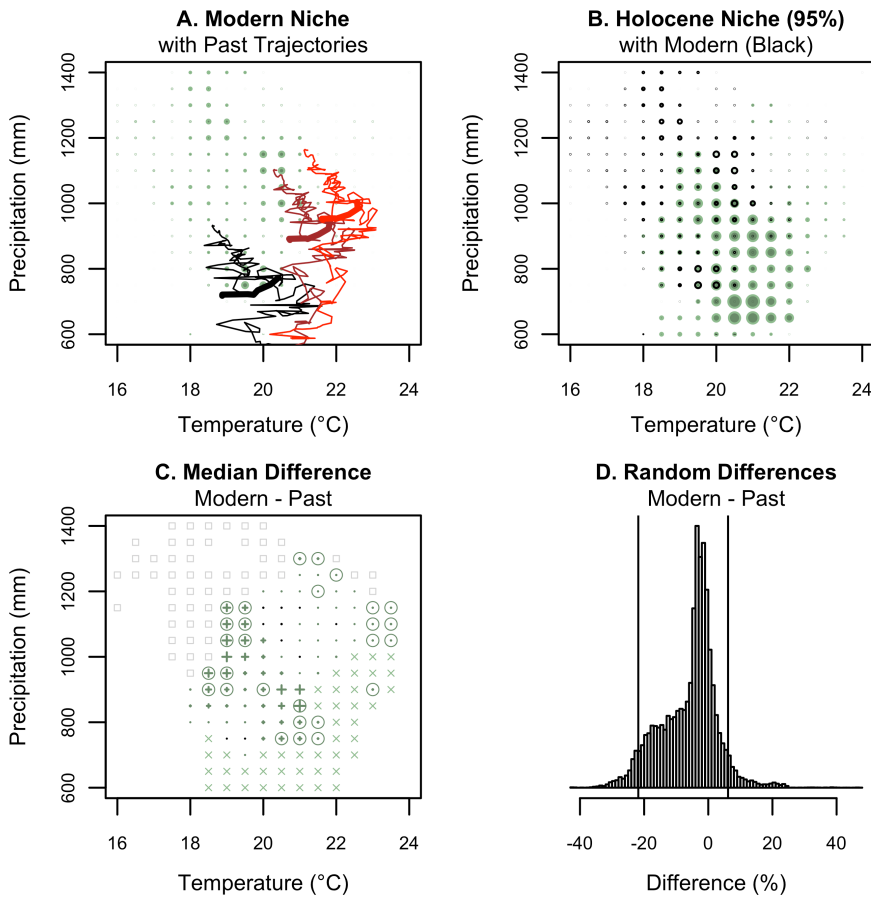


**Figure 5.** Plots show *Tsuga* pollen percentages today (A), during the Holocene (B), and their differences (C, D) with respect to mean July temperature and annual precipitation and the trajectories of three study sites (colored lines in A). Green circles indicate the upper 95% of the distribution of pollen percentages within 0.5°C and 50 mm windows with the largest symbols representing 50% *Tsuga* pollen. Modern pollen percentages also appear as black circles for comparison with green Holocene values in B. Panel A includes the climate trajectories of Knob Hill (black), Blood (brown), and Spruce ponds (red) with the period of rapid regional cooling at 5600-5300 YBP in bold. The lower end of each thin line represents the oldest samples; the right end of each bold line indicates 5600 YBP and the left end indicates 5300 YBP. Panel C shows the median differences between 1000 random pairs of modern and Holocene samples within each climate window: green plus symbols, scaled to the difference like the circles in A and B, indicate a greater median value during the Holocene than today. The few black symbols indicate the reverse. Circled symbols indicate significant differences. “X” denotes windows with non-zero Holocene medians but a zero median today; gray squares indicate modern climates not experienced by the study sites during the Holocene. The histogram in D shows the differences between all randomly paired samples with vertical black lines depicting the 95% range of differences.

## Running head: Hemlock responses to Holocene climates

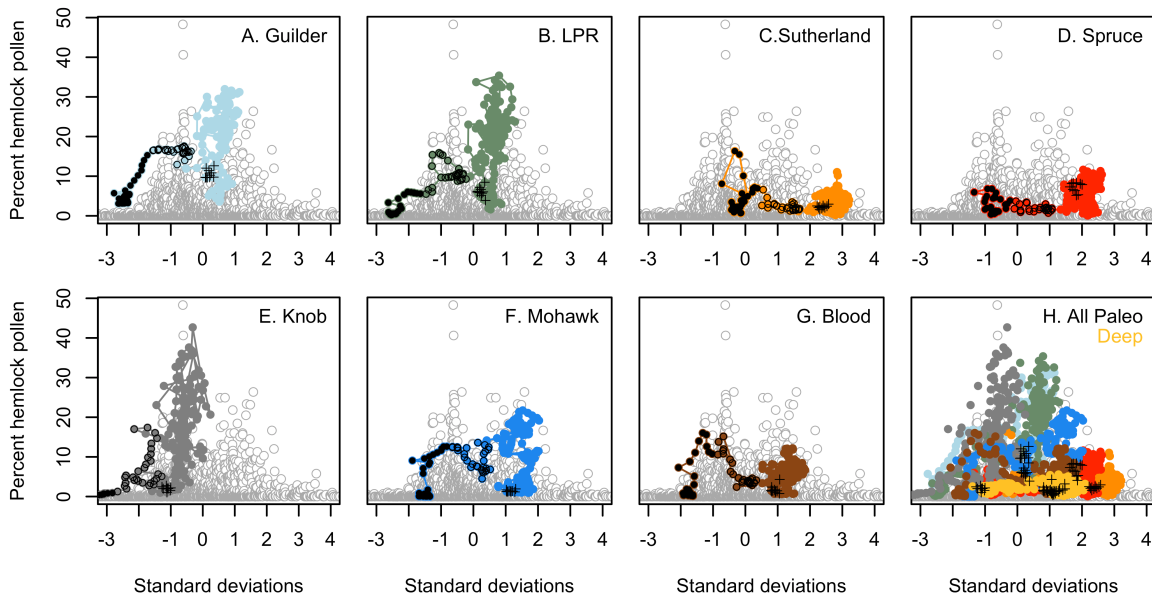


**Figure 6.** Fossil *Tsuga* pollen percentages from each study site (colored symbols) are plotted with respect to all modern samples (gray) and their climates, represented as standard deviations from the mean climate of all sites where *Tsuga* pollen percentages exceed 1% today (as in Figure 4B). Black circles represent samples older than 9000 YBP; black filled symbols represent >10,500 YBP and black outlined symbols, 10,500-9000 YBP. Black crosses indicate the 500-yr period after the decline from 5200-4700 YBP when percentages were low but retained bimodality (panel H). Because the regional climate became wetter through time (Fig. 2B), the oldest samples plot furthest left (negative departures from the mean) and the youngest samples to the right (positive departures from the mean). Sites shown are Guilder (light blue), Mohawk (dark blue), Sutherland (dark orange), Spruce (red), Knob Hill (dark gray), Little (LPR, dark green), Blood (brown), and Deep ponds (light orange). All sites are shown together in panel H. A supplementary animation shows the realized expression of these relationships by 500-yr time slice.

Running head: Hemlock responses to Holocene climates

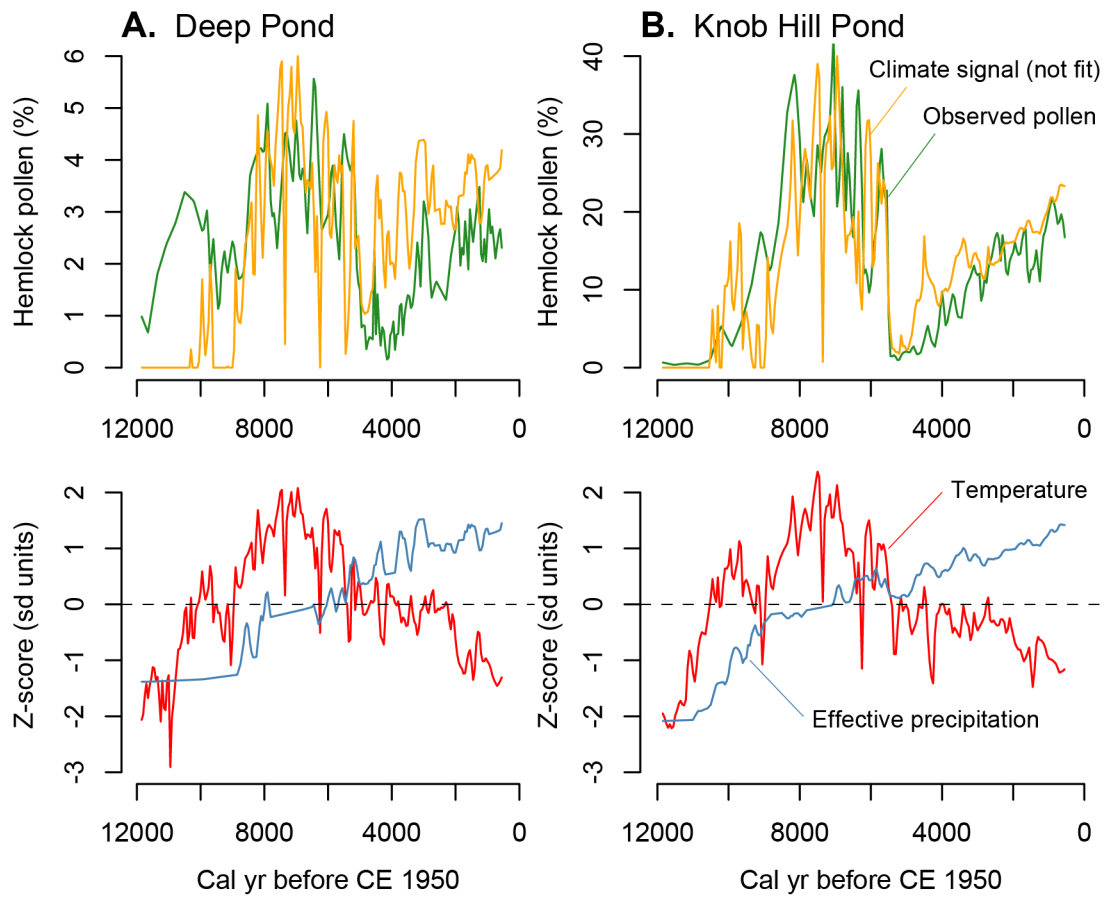


**Figure 7.** *Tsuga* pollen percentages from A) Deep and B) Knob Hill ponds (green) are shown with a climate index (orange) defined by the sum of the positive departures from the Holocene mean (z-scores) of July temperatures and annual precipitation for each site and scaled to the variance of the pollen data. The positive z-scores represent increases in either temperature or precipitation, like those represented by bold arrows in Fig. 3A, which would favor abundant *Tsuga*. The z-scores of the interpolated temperature (red) and precipitation (blue) series for each site are plotted versus time below.

## Running head: Hemlock responses to Holocene climates

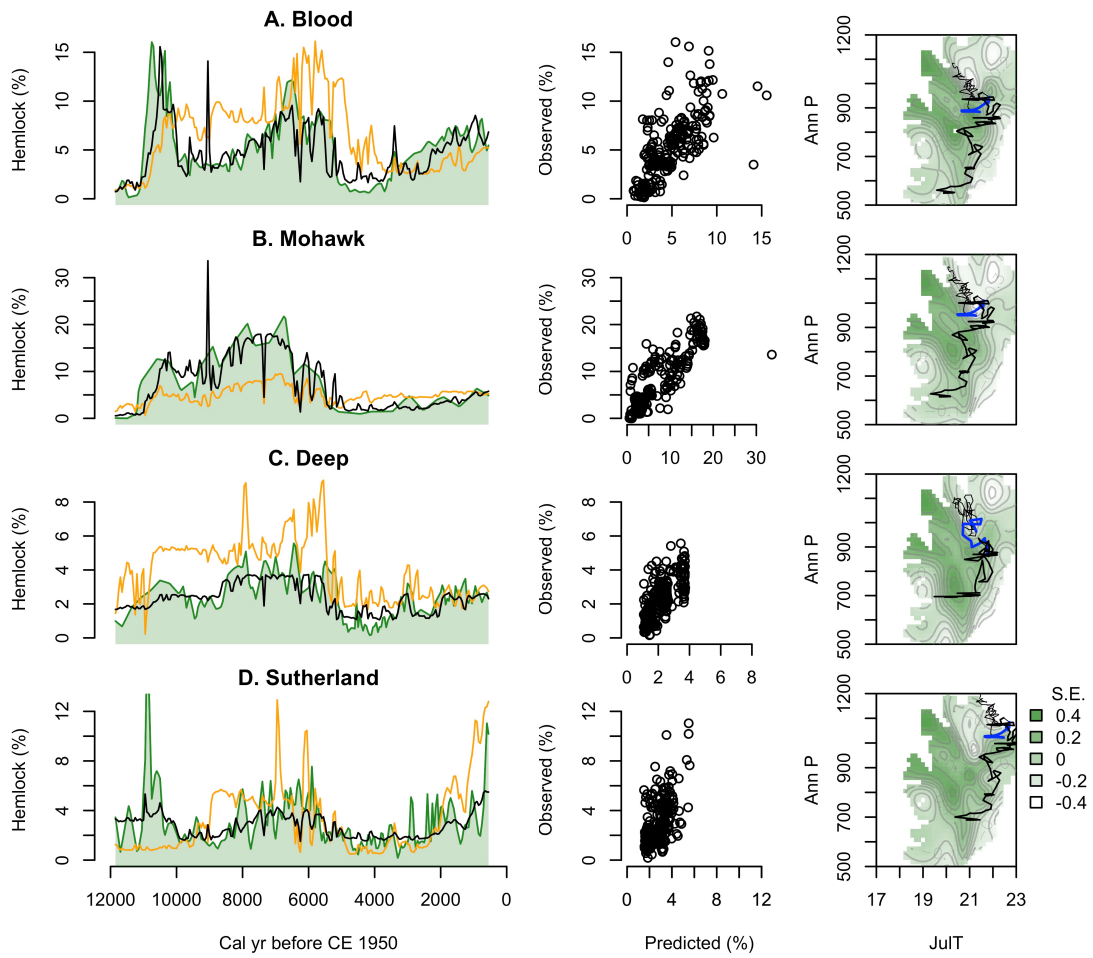


**Figure 8.** Comparison of observed *Tsuga* pollen percentages with site-specific and regional “leave-one-out” models for Blood, Mohawk, Deep, and Sutherland ponds. Left panels show the observed pollen percentages (in green) plotted versus time with the predicted values from both the site-specific (black) and “leave-one-out” (orange) GAMs. Scatter plots compare the observed and predicted values for each site-specific model. The right-most panels represent the response surface produced by fitting a GAMM to all data from >500 YBP in the region except for the target site. Contours represent increments of 0.1 standard error (S.E.) from the mean; light shades of green represent areas of low pollen percentages and dark shades represent areas of high percentages. Black lines show the climate trajectory of each individual site relative to mean July temperatures (JulT) and annual precipitation (AnnP) with blue line segments representing the period from 5600-5300 YBP associated with the classic *Tsuga* decline. Thin black lines represent the period after 5300 YBP whereas thick black lines represent the period before 5600 YBP.

## Running head: Hemlock responses to Holocene climates

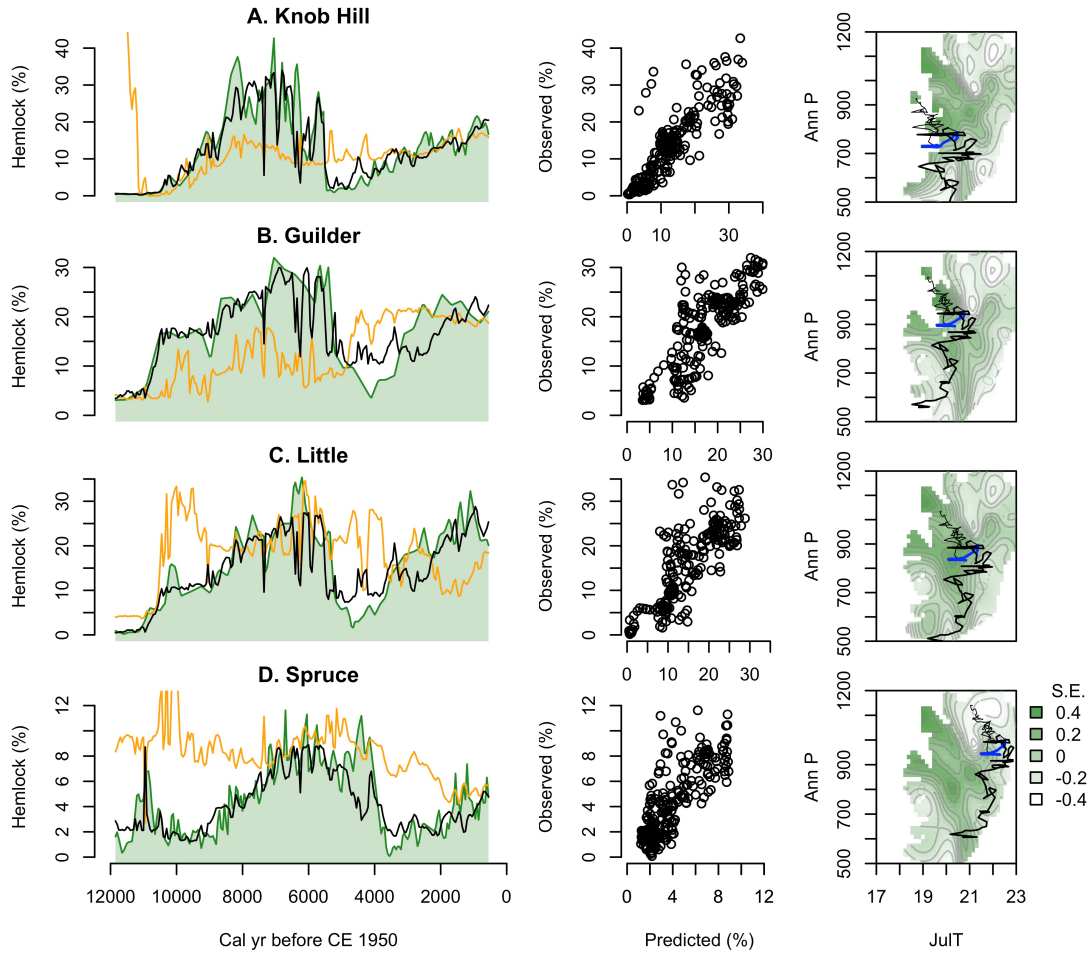


**Figure 9.** Same as Figure 8 but for study sites with deficient or erroneous regional “leave-one-out” models (Knob Hill, Guilder, Little, and Spruce ponds). Comparison of the surfaces in the right panels with those in Figure 8 or for Spruce Pond in D reveals truncated coverage, gaps, or misrepresentation of the bimodality in the models in A-C that target Knob Hill, Guilder, or Little ponds.

## Running head: Hemlock responses to Holocene climates

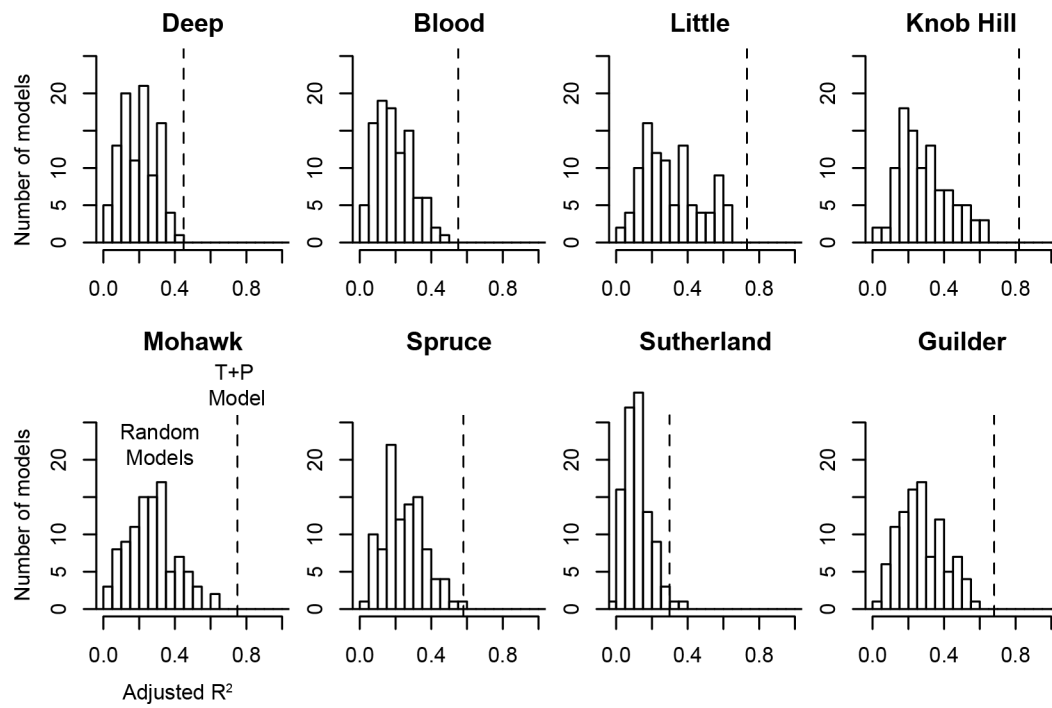


**Figure 10.** Histograms show the frequency of adjusted (Adj.)  $R^2$  values for GAMs generated for each site based on 100 pairs of random variables with the same temporal autocorrelation as the reconstructed temperature and effective precipitation time series used in the site-specific GAMs (black lines in Figures 8-9). The adjusted  $R^2$  for each site-specific (T+P) model, based on the actual climate reconstructions, is represented by a vertical dashed line.

## Running head: Hemlock responses to Holocene climates

### Appendix 1: Data and Method Details

#### Age models

We use the published age-depth relationships in calendar years for all study sites and records, and have made no chronological modifications. In this way, the data are presented as one possible distribution in time allowed by the radiocarbon age uncertainties associated at each site. When we discuss apparent agreement in timing of changes across records, we do so when the mean ages are similar and when even a formal analysis (Parnell et al., 2008) would not be able to rule out synchrony; fine-scale asynchrony within the age uncertainties (years to decades) can never be ruled out with the existing data. When we discuss differences in ages, we have used a formal analysis of synchrony based on the differences between 1000 random samples from the age uncertainty distribution, estimated using *bchron* (Haslett and Parnell, 2008), for each event to test whether the difference was significantly different from zero (Parnell et al., 2008). To enable comparisons across sites, all data were first linearly interpolated to even 50-year time steps. Ages of abrupt changes are based on the peak rates of change measured over 100-yr steps in the interpolated data. We focus on the interval from 550–11850 YBP because of the temporal limitations of the available temperature data (Sachs, 2007).

#### Paleoclimate records

The temperature time series used in our analyses represent growing-season SSTs off the coasts of Nova Scotia (core OCE326-GGC30; Sachs, 2007) and Virginia (core CH0798-GGC19; Sachs, 2007), which we assume to also represent regional trends in

## Running head: Hemlock responses to Holocene climates

mean July temperatures of this coastal region. Data from Nova Scotia derive from the region of the Labrador Current, which supplies the Gulf of Maine to the east of New England; data from Virginia derive from the region of the Gulf Stream, which transports heat north along the southern coast of New England. The temperature anomalies are interpolated to the locations of the pollen records based on site latitude to account for mixing of the northern and southern temperature signals; the results build on the high degree of spatial autocorrelation expected for temperature across the region.

Following Shuman and Marsicek (2016), each SST reconstruction was linearly detrended to account for a large trend in the data (e.g., equal to cooling of  $>5^{\circ}\text{C}$  since 11,000 YBP in core GGC30), which may be driven by non-climatic controls on alkenone production (Prahl et al., 2006). Without detrending, New England temperatures during the cold Younger Dryas interval (before 11,700 YBP) and other parts of the Pleistocene would have been as high as those in modern day North Carolina, which is inconsistent with terrestrial stable isotope records (Huang et al., 2002; Kirby et al., 2002; Hou et al., 2006; Zhao et al., 2010) and the region's ecological history (e.g., boreal forests in Massachusetts at 12,000 YBP). The detrended signal (Fig. 2A) aligns well with elevational changes in tree species distributions known from plant macrofossils in the White Mountains, New Hampshire and the Adirondacks, New York (Spear, 1989; Jackson and Whitehead, 1991; Spear et al., 1994; Shuman et al., 2004) and with pollen-inferred temperatures for the region (Webb III et al., 1993; Marsicek et al., 2013). The detrended SST records also contain multi-century variability that correlates significantly with variations in the independently derived effective moisture records (Shuman and Marsicek, 2016).

## Running head: Hemlock responses to Holocene climates

Effective precipitation (precipitation minus evapotranspiration) was derived from reconstructed lake-level changes at Davis Pond in western Massachusetts (Newby et al., 2011, 2014) and Deep Pond on the southern coast of Cape Cod, Massachusetts (Marsicek et al., 2013; Newby et al., 2014). At each site, transects of sediment cores were used to constrain past shoreline position, which we converted to effective precipitation using a simple water budget model for each lake and watershed (Marsicek et al., 2013; Pribyl and Shuman, 2014). Interpolation of the effective precipitation signals from Deep and Davis ponds to the location of the pollen records was carried out based on longitude because of the east-west orientation of the available records (Fig. 1A). The timing of changes in each record is constrained by >3 cores and 31-53 calibrated radiocarbon ages (Newby et al., 2014). As with the pollen and alkenone-derived SST data, no modifications were made to the published age-depth relationships, which were derived using *bchron* (Haslett and Parnell, 2008; Newby et al., 2014).

### Generalized Additive Models (GAMs)

To evaluate the variance in the pollen data explained by the climate reconstructions, we use generalized additive mixed models. They were applied after the pollen percentages were square-root transformed to ensure a normal distribution. The GAMs, thus, take the form  $Tsuga^{0.25} = \text{function (July Temperature, Annual Precipitation)}$ , and were applied using a tensor product smooth using a cubic regression spline, Gaussian error distribution, and an identity link function in the *mgcv* package in R (Wood, 2006b; Wood, 2011; R Core Development Team, 2017). We used analysis of variance (ANOVA) to compare various models such as those with additive versus interactive

## Running head: Hemlock responses to Holocene climates

predictors, spline versus tensor product smooths, cubic regression versus thin plate regression for each marginal basis, and the inclusion of site as a random effect; the model choices represented the lowest residual degrees of freedom.

To further ensure that the GAMs do not represent spurious correlations common to autocorrelated time series (Granger and Newbold, 1974), we also generated 100 random time series with the same temporal autocorrelation structure as observed in temperature and moisture reconstructions. The approach was inspired by analyses of significance in paleoenvironmental reconstruction by Telford and Birks (2011), and random number series were generated using the function, *gstat*, in R.

### Sources of error

Uncertainty in our analyses stems from factors such as the limits to how well the existing paleoclimate data represent the region, the age uncertainties of the records, the simplified linear interpolation of the climate reconstructions, and the detrending of the SST reconstructions. The alternative GAMs generated using random time series (Fig. 10) indicate that the climate reconstructions must have captured accurate, non-random climate signals to suitably predict the pollen percentages through time even if some errors in absolute climates or ages exist. The long-term negative correlation between temperature and precipitation, as well as the abrupt changes in the SST record at ca. 5500 YBP, exist in the data whether or not we detrend the SSTs. The major differences between the detrended and non-detrended temperature schemes center on the period before ca. 7000 YBP. Therefore, the role of temperature in the *Tsuga* decline is unlikely to derive from our treatment of the temperature data.

## Running head: Hemlock responses to Holocene climates

The roles of winter temperatures or seasonal precipitation have not been well constrained and could also modify the specific climate effects detected here. Covariance of climate variables could have translated winter signals to either summer temperature or annual precipitation in our models. Likewise, ocean temperatures, likewise, may not represent the regional air temperatures (although see Shuman and Marsicek 2016). Errors could also arise from our assignment of absolute temperature and precipitation values based on different base periods in the 20<sup>th</sup> century, but sensitivity analyses indicate that the major patterns discussed here are not substantially affected by using a different base period.